Proceedings of the 11th Australian Space Science Conference Canberra 26 - 29 September, 2011

Australian Space Science Conference Series

1st Edition
Published in Australia in 2012 by
National Space Society of Australia Ltd
GPO Box 7048
Sydney NSW 2001
Fax: 61 (02) 9988-0262
email: nssa@nssa.com.au
website: http://www.nssa.com.au

ISBN 13: 978-0-9775740-5-6

Editors: Wayne Short and Iver Cairns

Distributed on DVD

Table of Contents

List of Proceedings Papers

List of Proceedings Papers

List of Proceedings Papers

The initial - INtegrated SPectrograph, Imager and Radiation Explorer (i-INSPIRE) - a university satellite project.

Lisa Fogarty*, Iver Cairns*, Joss Bland-Hawthorn*, Xiaofeng Wu†, Chris Betters*, Jiro Funamoto†, Sergio Leon-Saval*, Tony Monger*, Size Xiao†

* *School of Physics, A28, University of Sydney, NSW, 2006, Australia*
† *School of Aerospace, Mechanical and Mechatronic Engineering, University of Sydney, NSW, 2006, Australia*

Summary: i-INSPIRE (initial-INtegrated SPectrograph, Imager and Radiation Explorer) is a collaborative project at the University of Sydney combining expertise from the School of Physics and the School of Aerospace, Mechanical and Mechatronic Engineering. i-INSPIRE is a small, light-weight, tube-shaped satellite which will be the first of its kind to be fully constructed and operated by an Australian university. This paper overviews the underlying concepts and aims of the i-INSPIRE project, describes the satellite and its sub-systems, gives an introduction to the science instruments, and posits some future directions for space-based projects at the University of Sydney.

Keywords: Satellite, photonics, spectrograph, radiation counter, imager.

Introduction

The initial - INtegrated SPectrograph, Imager and Radiation Explorer (i-INSPIRE) is a collaborative project between the School of Physics and the School of Aerospace, Mechatronic and Mechanical Engineering at the University of Sydney. It is a pico-satellite (<1 kg) which will be the first to be built, launched and operated by a single Australian university. The project is envisioned as a demonstration of the capability of the University of Sydney collaboration, and the Australian university community in general, to successfully launch and operate satellites.

The i-INSPIRE satellite is the first step towards the development of an Australian near-Earth space capability as recommended in the Decadal Plan for Australian Space Science [1]. As such i-INSPIRE is considered a crucial step towards the realisation of the Marabibi constellation. The Decadal Plan focusses on linking such diverse science areas as astronomy, Earth science and climate change (for example) within the context of space-based missions and their associated data-gathering capabilities. To this end the Decadal Plan also recommends the development of new instruments suitable for space, making specific mention of the huge potential of advanced photonic instrumentation. The science payload on board i-INSPIRE includes a novel photonic micro-spectrograph called NanoSpec (described in more detail below and in Betters et al. [2]).

From a technical point of view, the project aims to demonstrate the successful building, testing, and operation of the i-INSPIRE satellite and its sub-systems. A vital part of this is the development of software to co-ordinate the operation of the science instruments, the storage

of science data and basic telemetry, and the operation of the satellite transceiver. We must also be able to communicate with i-INSPIRE from the ground. This involves building and operating a suitable ground station, the purpose of which is to transmit signals to the satellite, to receive signals from the satellite, and to store all data from the satellite. An associated system is envisioned to decode, process, and analyse the data offline. This entire system is hereafter referred to as the ground station. The technical aspects of i-INSPIRE are laid out in more detail in Funamoto et al. [3] and Xiao et al. [4].

As well strategic and technical aims, i-INSPIRE also has science goals. The satellite carries a photonic micro-spectrograph (NanoSpec), a small imaging camera and a radiation counter (see below and Betters et al. [2] for a more detailed description of the instruments). NanoSpec is fed with eight optical fibres which point along four different directions out of the spacecraft. Light will couple to the fibres from any bright objects at which the spacecraft happens to 'point' during its orbit. NanoSpec will therefore record spectra of the Earth, Sun, and possibly some stars. The spectra of the Earth should allow land and sea to be distinguished. NanoSpec will also record Cerenkov radiation caused by high-energy particles passing through the fibres. This enables us to study the effects of such radiation on the performance of optical fibres and thereby assess the hardiness of photonic instruments in space. We will also be able to correlate the Cerenkov events recorded by NanoSpec with the data from the radiation counter. We expect to see more Cerenkov events when passing through regions of higher radiation.

The purpose of the radiation counter is to probe the radiation environment in low Earth orbit. The radiation counter will detect radiation from the Earth's radiation belts and magnetosphere as well as the Sun, and galactic cosmic rays. In addition i-INSPIRE will pass through the South Atlantic anomaly[1] every 16 orbits. We expect robust detection of the South Atlantic anomaly and of transient space weather events [5]. These data will allow us to construct time-varying radiation maps of the Earth.

The imaging camera is placed so that its lens points outside the satellite body. The camera will take photographs of its surroundings at regular intervals. Since i-INSPIRE is unable to control its attitude the images from the camera will be useful in determining the parameters of the tumble of the satellite within its orbit. At some point in the 24-day mission it is hoped that the camera will photograph Australia from space, providing us with the first images of Australia captured by an entirely Australian satellite.

The Satellite

The i-INSPIRE satellite is a tube shaped pico-satellite with a maximum mass of 0.75 kg. The satellite has a maximum height of 127 mm and a maximum diameter of 92.5 mm. The outer structure of the satellite is supported by a frame of aluminium strips alternating with solar cells. The solar cells are used to charge a lithium-ion (Li-ion) battery which powers all the satellite systems and science payloads. A photograph of the assembled satellite body is shown in Fig. 1. This type of satellite is similar in mass and size to the popular 'CubeSat' and has therefore acquired the sobriquet 'TubeSat'[2].

[1]The South Atlantic anomaly is a known region of high radiation occurring at the point where the Van Allen radiation belts are closest to the Earth.

[2]see: http://interorbital.com/TubeSat_1.htm

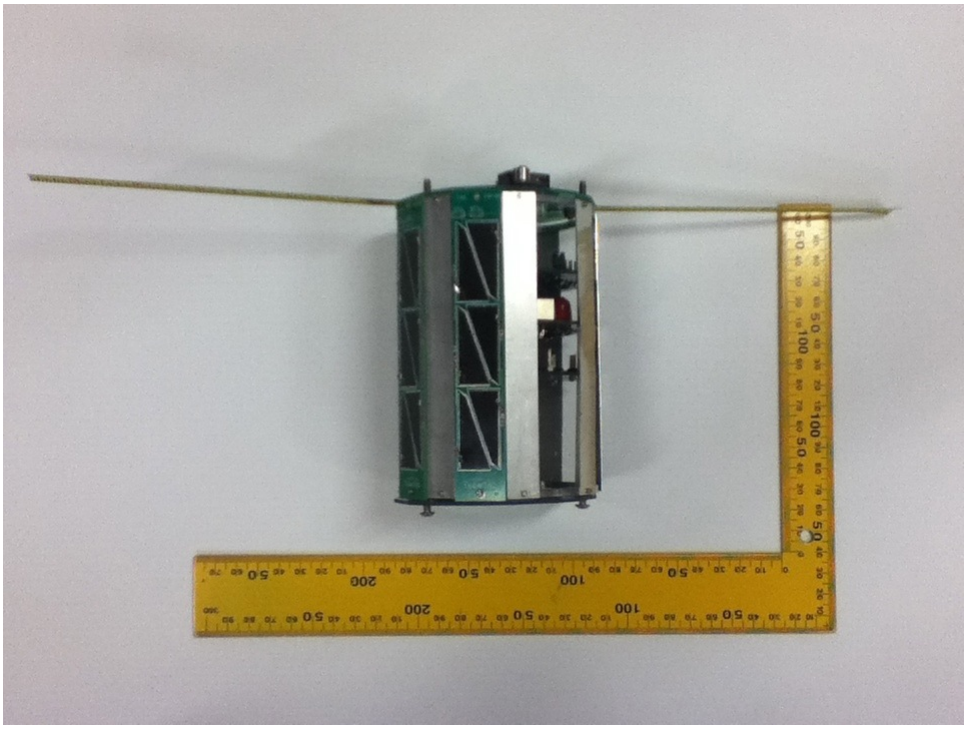

Fig. 1: A photograph of the i-INSPIRE satellite body.

The satellite carries a 3.7 V, 5.2 A hr battery to supply power to all satellite sub-systems. A power board transforms the input voltage from this battery to the various voltages used by the other parts of the satellite. The main satellite sub-systems are the micro-controller, the transceiver, the data storage chip, and the science instruments. For more information on the satellite bus design see Xiao et al. [4]

The micro-controller is a BasicX-24 chip and is the heart of the satellite. It is used to interface all other active parts of the satellite. All data from the instruments are processed and stored by the micro-controller, either in the memory of the micro-controller itself, or in the data storage chip (this is a micro-SD card connected to the BasicX-24). The micro-controller also commands the transceiver. All these tasks are handled by the main program (written in BasicX) which runs on the micro-controller.

The transceiver is a Radiometrix TR2M coupled with a Radiometrix AFS2 amplifier chip. The transceiver transmits and receives signals at 433 MHz. The University of Sydney has a ground station designed to receive the data transmitted by i-INSPIRE.

The ground station can only communicate with the satellite when the satellite is within a certain range of the ground station. In the proposed orbit this will occur about four times a day and for an average duration of 5 minutes per occurrence (see the below Section entitled "The Launch" and Funamoto et al. [3]). Since the maximum data downlink rate is 5 kbit/s, only a strictly controlled amount of data can be downloaded during each period of contact with the spacecraft.

The Instruments

Of the three instruments i-INSPIRE carries in its science payload, the largest and most complex is NanoSpec, a novel photonic micro-spectrograph. "Photonics" is the area of research dealing with guided light in devices such as optical fibres or new inventions like photonic lanterns [6]. The field of "astrophotonics" uses photonic techniques in the design and construction of astronomical instruments. These instruments are in turn used to observe astrophysical or solar system sources. Astronomical instruments designed with photonic elements can be very light-weight and compact making "space photonics" a natural extension of the concepts involved in astrophotonics: photonic instrumentation is clearly well-suited to space applications where both the size and weight of satellites are strictly limited. For more information on the development and growth of space photonics see Leon-Saval and Bland-Hawthorn [7]. NanoSpec is a high resolution spectrograph based on the PIMMS concept [8]. PIMMS is a unique idea which uses innovations in photonics to achieve high resolution spectroscopy using a very light-weight and compact device.

Most astronomical instruments are built using multi-mode fibres (MMFs), that is optical fibres that allow propagation of light in many spatial modes. The number of propagating modes depends on the physical size of the fibre and the wavelength of the light. By contrast, single-mode fibres (SMFs) allow propagation of light in a single spatial mode with a Gaussian shape. One of the limiting factors in achieving high resolution spectroscopy is the physical size of the input to the spectrograph itself (in astronomy this is usually referred to as the slit width, since the input to an astronomical spectrograph is usually arranged in the form of a slit). When using MMFs, which are popular in astronomy due to the relative ease of coupling light into the fibre itself, the slit width can be hundreds of microns in size. For the same wavelength of light SMFs can be as small as three microns, making the theoretical limit of spectral resolution achievable in an SMF device. The downside to this it is much more difficult to couple light to a physically small fibre and so an SMF device will have lower throughput than a comparable MMF device.

NanoSpec is a proof-of-concept SMF-based PIMMS spectrograph. The spectrograph is small (roughly $40\,\mathrm{mm} \times 40\,\mathrm{mm} \times 60\,\mathrm{mm}$), light-weight, and constructed with off-the-shelf components. Nanospec is directly fed with eight SMFs that point in four directions outside the spacecraft. It is hoped that light will couple into NanoSpec from the Earth (enabling the measurement of spectra of both land masses and oceans), from the Sun, moon, and potentially stars. It is also hoped that NanoSpec will measure Cerenkov radiation in the SMFs generated by particular radiation passing though the SMF.

A CAD model and photograph of NanoSpec are show in Fig. 2. NanoSpec was built and tested in the astrophotonics laboratory in the School of Physics at the University of Sydney. The theoretical maximum spectral resolution for NanoSpec is calculated to be $\mathrm{R} = \lambda/\Delta\lambda \simeq 1080$. The measured resolution was found to be $\mathrm{R} \simeq 920$, very close to the theoretical maximum and impressive for such a compact device. For more details on the design, construction, and testing of the initial version of NanoSpec see the companion paper of Betters et al. [2].

i-INSPIRE also carries an off-the-shelf imaging camera. The compact device is manufactured by LinkSprite and is shown in Fig. 3. The lens of this miniature camera is placed so that it points outside the satellite. It will take photographs of the environs of i-INSPIRE at a regular (and yet to be determined) time interval. These photographs serve a two-fold purpose. Firstly,

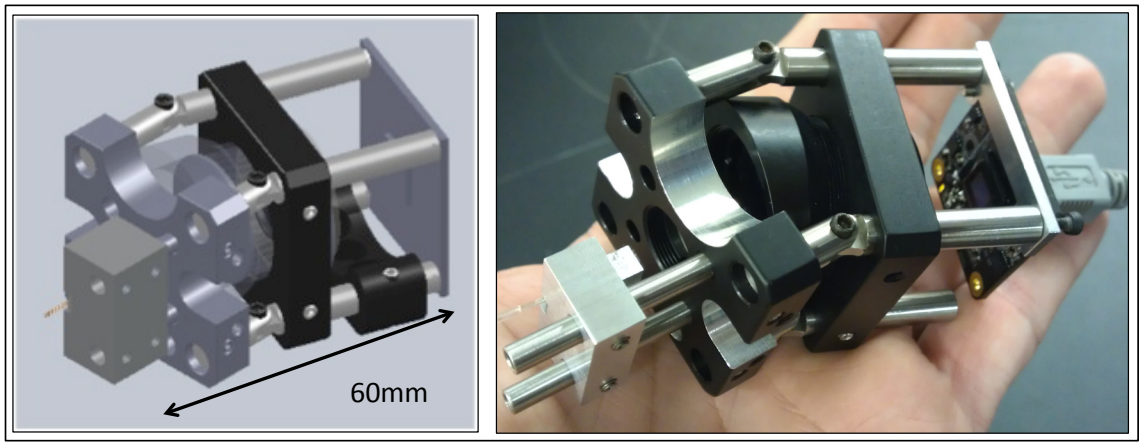

Fig. 2: The left-hand panel shows a CAD model of NanoSpec. The right-hand panel shows a photograph of the device. As can be seen NanoSpec is a very compact instrument, fitting comfortably in the palm of the hand.

i-INSPIRE should capture some images of Australia and its surrounding oceans, making these the first images of Australia taken by an Australian spacecraft. Secondly, the images should allow the tumbling of the satellite in its orbit to be reconstructed. Since i-INSPIRE has no active attitude determination or control capability this is an invaluable addition to the science payload.

Fig. 3: The LinkSprite colour camera which will form part of the i-INSPIRE payload.

The third science instrument is a radiation counter. We currently plan to fly a Geiger tube based on off-the-shelf components but modified to fit within our tight space constraints (see Betters et al. [2]). The radiation counter will continuously detect energetic particles from the Earth's radiation belts and magnetosphere, the Sun and cosmic rays. We aim to characterise the spatially and temporally varying radiation environment through which i-INSPIRE traverses. We hope to create radiation maps of the Earth at 310 km altitude, with a robust detection of the South Atlantic anomaly and of space weather events [5]. These maps can then be correlated with signatures of Cerenkov radiation seen by NanoSpec.

The Launch

i-INSPIRE is scheduled to be launched in 2012 on a Neptune 45 (N45) rocket developed by a United States company called Interorbital Systems (IOS). The launch is expected to take place off the coast of California. IOS are currently completing tests on the launch vehicle and finalising their launch certification.

The N45 rocket is a three-stage rocket formed of seven identical propulsion modules clustered together and firing at different stages in the launch, as can be seen in Fig. 4. The rocket is capable of launching 45 kg into a low earth polar orbit at a height of 310 km, for instance carrying 32 TubeSats and 10 CubeSats.

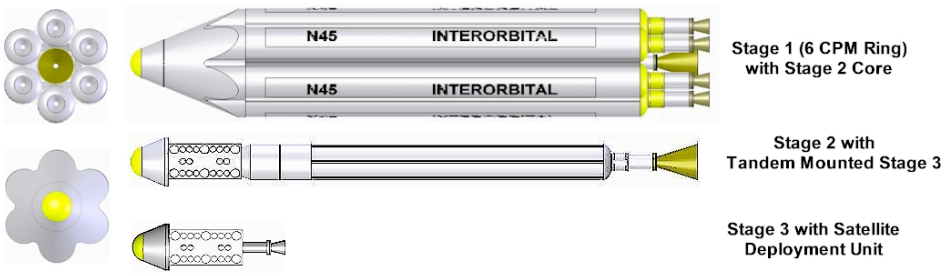

Fig. 4: A diagram showing the three-stage N45 rocket developed by IOS

The satellite orbit should have a 90 minute period, implying 16 orbits can be completed in one day. i-INSPIRE employs line-of-sight communications and so must pass over Australia, the location of the ground station, in order to downlink its data. In the proposed orbit this occurs four times a day and for an average duration of five minutes at a time, giving the satellite about twenty minutes a day in which to downlink data. For a more detailed description of the orbital parameters see Funamoto et al. [3].

Conclusions

i-INSPIRE is a small TubeSat being built and launched by a collaboration between the School of Physics and the School of Aerospace, Mechatronic and Mechanical Engineering at the University of Sydney.

It is a pilot project aimed at developing a rich and sustainable level of space expertise at the University of Sydney. The overall aim of the project is to demonstrate the ability of an Australian university group to design, build, and operate space-based projects. i-INSPIRE is the first step towards an Australian low Earth orbit space capability, as recommended by The Decadal Plan for Australian Space Science [1].

A novel new micro-spectrograph called NanoSpec will be flown. Based on innovative photonic technology, NanoSpec breaks new ground by demonstrating high-resolution spectroscopy in an extremely compact and light-weight device. NanoSpec is also a crucial test of the space-hardness of fibre optics and other photonic technologies. i-INSPIRE also aims to be the first entirely Australian-owned and -operated satellite to photograph Australia from space. We also hope to create a radiation map of the world in a low Earth orbit (c. 310 km

altitude), with a robust detection of the South Atlantic anomaly and of space weather events [5].

The i-INSPIRE project may also be a springboard to other Australian and international space projects. These are not restricted to satellite launches and may include other ventures such as testing potential payloads on weather balloons or partaking in much larger and longer-lived balloon experiments.

References

[1] I. Cairns, M. Baltuck, B. Biddington, R. Boswell, R. Boyce, G. Caprarelli, J. Clarke, D. Cole, P. Dyson, B. Fraser, A. Held, M. Norman, C. Oliver, A. Parfitt, C. Rizos, P. Robinson, A. Rozenfeld, R. Vincent, M. Walter, C. Waters, P. Wilkinson, and J. Zillman, *Decadal Plan for Australian Space Science: Building a Presence in Space*, 2009.

[2] C. Betters, I. Cairns, J. Bland-Hawthorn, X. Wu, L. Fogarty, J. Funamoto, S. G. Leon-Saval, T. Monger, and S. Xiao, "Instrumentation of the i-INSPIRE satellite." in *Proceeding of the 11th Australian Space Science Conference*, 2011.

[3] J. Funamoto, I. Cairns, J. Bland-Hawthorn, X. Wu, C. Betters, L. Fogarty, S. G. Leon-Saval, T. Monger, and S. Xiao, "Engineering i - INSPIRE - a pico-satellite from Australia." in *Proceeding of the 11th Australian Space Science Conference*, 2011.

[4] S. Xiao, X. Wu, I. Cairns, J. Bland-Hawthorn, C. Betters, J. Funamoto, S. G. Leon-Saval, L. Fogarty, T. Monger, and X. Bai, "i - INSPIRE Tube-Satellite Bus Design." in *Proceeding of the 11th Australian Space Science Conference*, 2011.

[5] K. Scherer, H. Fichtner, B. Heber, and U. Mall, Eds., *Space Weather: The Physics Behind a Slogan*. Springer, 2005.

[6] S. G. Leon-Saval, T. A. Birks, J. Bland-Hawthorn, and M. Englund, "Multimode fiber devices with single-mode performance," *Opt. Lett.*, vol. 30, no. 19, pp. 2545–2547, Oct 2005. [Online]. Available: http://ol.osa.org/abstract.cfm?URI=ol-30-19-2545

[7] S. G. Leon-Saval and J. Bland-Hawthorn, "Space Photonics: next generation space instrumentation." in *Proceeding of the 11th Australian Space Science Conference*, 2011.

[8] J. Bland-Hawthorn, J. Lawrence, G. Robertson, S. Campbell, B. Pope, C. Betters, S. Leon-Saval, T. Birks, R. Haynes, N. Cvetojevic, and N. Jovanovic, "PIMMS: photonic integrated multimode microspectrograph," in *Society of Photo-Optical Instrumentation Engineers (SPIE) Conference Series*, ser. Society of Photo-Optical Instrumentation Engineers (SPIE) Conference Series, vol. 7735, Jul. 2010.

Instrumentation of the i-INSPIRE satellite.

C. Betters[1,3], I. H Cairns[1], J. Bland-Hawthorn[1], X. Wu[2], L. Fogarty[1], J. Funamoto[1,2], S.G. Leon-Saval[1], A. Monger[1] and S.Z. (A.) Xiao[2]

[1] *School of Physics, Building A28, University of Sydney, NSW, Australia, 2006*
[2] *School of Aerospace, Mechanical and Mechatronic Engineering, Building J07, University of Sydney, NSW 2006*
[3] *Corresponding author: c.betters@physics.usyd.edu.au*

Summary: The i-INSPIRE (initial - INtegrated SPectrograph, Imager and Radiation Explorer) pico-satellite is intended to be Australia's first University satellite to be launched and operated in space. It will carry a novel photonics-based spectrograph (NanoSpec), an imaging camera, and a radiation counter. NanoSpec is a single mode fibre-fed spectrograph operating very close to the diffraction limit with a nominal spectral resolution of 0.5 nm. The primary goal of NanoSpec is to demonstrate the potential of photonics-driven technology in space-based applications. To that end it will obtain the first spectra from a space-borne, photonics-based spectrograph. These spectra will be used to identify features related to the Earth and Sun and determine the effects of radiation events on the device. Additionally the satellite will carry a radiation counter to obtain a radiation map of the Earth while in orbit, for correlation with NanoSpec data and space weather events, and an imaging camera to deliver the first photographs of Australia from an entirely Australian-owned and -operated spacecraft.

Keywords: diffraction limited spectroscopy, TubeSat, pico-sat, astrophotonics, micro-spectrograph

Introduction

The i-INSPIRE satellite project is a collaboration between the School of Physics and the School of Aerospace, Mechanical and Mechatronic Engineering at the University of Sydney. We intend for i-INSPIRE to be the first sole Australian university satellite to be launched and operated in space (cf. Ref [1], for a more detailed overview of the aims of the mission). On board we will demonstrate a novel spectrograph, dubbed NanoSpec, which uses state of the art photonic techniques. To complement the spectrograph the satellite will also carry an imager and radiation counter.

The satellite subsystems are based upon the 'TubeSat' design sold as part of a launch package with start-up Interorbital Systems[1] (IOS; cf. Ref [2]). The i-INSPIRE satellite is one of 32 TubeSats and 10 CubeSats currently on the manifest for the maiden launch of IOS's N45 rocket. The targeted orbit is a high inclination polar orbit with an altitude of 310 km and a predicted lifetime of ~24 days (>380 orbits). Approximately every 16 orbits the satellite will move through the South Atlantic anomaly (SAA), a region of high radiation. This region is of particular interest, as it will allow us to study the short-term effect of radiation on NanoSpec's components and to detect associated Cerenkov light. Here we first discuss the expected radiation environment in orbit and its implications for the spectrograph design and the radiation counter. Specifically, we investigate the possible generation of Cerenkov radiation in the optical fibre feed and radiation induced errors in the spectrograph components. We then introduce the design of NanoSpec, and present preliminary results on the engineering

[1] http://www.interorbital.com/

version's performance. In the remaining sections we provide an overview of the imaging camera, closing with a discussion of future plans and possibilities.

Radiation environment

The radiation environment in a terrestrial orbit is complex but can be modelled as a combination of galactic cosmic rays (GCRs), particles trapped in the Earth's magnetic field (also known as trapped radiation or the Van Allen belts; lower energy particles, <10MeV are due to magnetospheric sub-storms) and energetic solar particle events (ESPs) such as flares or coronal mass injections (CMEs). The radiation environment in low earth orbit (LEO) is further complicated by interactions with the Earth's magnetic field, resulting in a radiation flux that will vary strongly with time, altitude, orbital inclination and orientation with respect to the sun [3].

In the orbit anticipated for i-INSPIRE[2] the effects of trapped radiation dominate the radiation environment, so in this discussion we ignore other contributions. *Figure 1* show the average flux of protons and electrons over a 24 day period according to the NASA AP8 and AE8 trapped radiation models for both solar maximum and minimum [4] (calculated using SPENVIS [5, 6] and CREME96 [7] codes). AP8 models the proton component of trapped radiation belts in orbit, while the AE8 is the electron component. The solar cycle is an important factor in both the AP8 and AE8 models as it leads to attenuation in the intensity of trapped protons and an increase in the intensity of trapped electron radiation. This is due to the enhanced magnetic turbulence in the solar wind near a solar maximum. The current solar cycle (24) is predicted to reach a maximum in May 2013, however it is projected to be weaker then average [8]. We thus expect the actual environment seen by the i-INSPIRE satellite in 2012 will be within the region bound by the AP8 and AE8 max and min curves seen in Fig. 1.

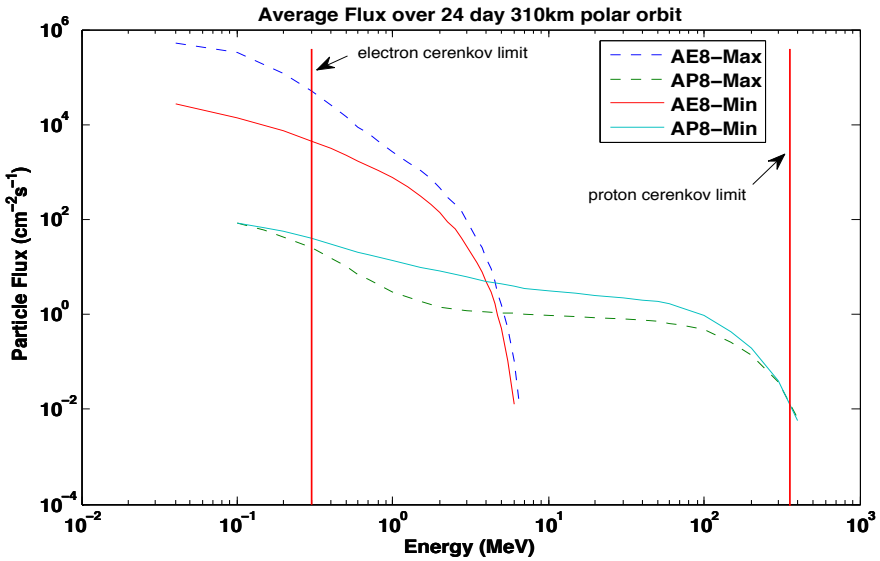

Figure 1 - The flux of electrons and protons in 310 km LEO according to the AP8 and AE8 radiation belt models respectively. The attenuation of proton flux below 1 GeV by the solar wind can also be seen as a reduced flux during solar maximum [5, 6, 9]. The opposite can be seen for electron flux, which increases by up to an order of magnitude during solar maximum. The red bars indicate the energy required for the respective particle to be travelling faster then the 0.7 times the speed of light.

[2] High inclination orbit with an altitude of 310km

Additionally, there are two hot spots of activity: at the poles, where electron precipitation is highest; and at the South Atlantic anomaly, where the inner radiation belt is closest to the earth's surface. It is in these regions we expect any radiation effect to present themselves in NanoSpec and the control systems.

Radiation Counter

To track the radiation level during an orbit, we have included a Geiger tube based radiation counter as one of the instruments on i-INSPIRE. The current design is based upon an open source design from 'SparkFun Electronics, CO, USA'. We have removed, replaced and reorganised components of the electrical and printed circuit board (PCB) design to be compatible with the restricted space available in the TubeSat and relatively harsh environment of space. Testing is currently underway to ensure the final component will function in orbit and survive launch. Using the radiation data collected we hope to build a radiation map of LEO consistent with models (i.e. AP8 and AE8) and correlate this with data collected by the spectrograph.

Implications

The i-INSPIRE TubeSat does not have significant shielding against any form of radiation, so we must consider the implications that the LEO radiation environment will have for the instruments. Besides single event upset (SEU) occurrences that can cause the computer or detector to malfunction, we are most concerned with the possibility of Cerenkov light being generated in the optical fibre feed of NanoSpec. Cerenkov radiation is commonly pictured as the blue glow seen around submerged nuclear reactors, but is also central to many particle, astrophysics and space experiments [10, 11]. If radiation is generated in an optical fibre it can be trapped and subsequently dispersed in the spectrograph, thereby decreasing the signal to noise ratio of any detected spectra. This effect has been documented in medical physics studies where optical fibres used in radiation dosimetry are exposed to therapeutic particle beams [12, 13].

Coupling of Cerenkov in optical fibres

Cerenkov photons are emitted when charged particles travel faster then the local speed of light in a material. These photons are emitted at angle θ with respect to the direction of travel forming the characteristic Cerenkov cone Fig. 2a. In the optical fibre feed of NanoSpec this translates to particles traveling faster then 0.7 times the speed of light in vacuum and an angle θ between $10-47°$ degrees. The red lines in Fig. 1 mark the minimum energy for electrons (~ 0.2 MeV) and protons (~ 0.38 GeV) to satisfy this condition.

Ref [14] quantifies the effect of Cerenkov radiation on a signal in an optical fibre, calculating the fraction of a Cerenkov cone that couples in to guiding modes. Eqn. 1 describes the intensity of Cerenkov light coupled into a fibre due to a single particle,

$$I_{coupled} \propto \underbrace{\left(\frac{2r}{\sin\alpha}\right)}_{1}\underbrace{\left(\frac{1}{\pi}\frac{v\left(n-\Delta n\right)-c\cos\alpha}{\sin\alpha\sqrt{nv^2-c^2}}\right)}_{2}\underbrace{\left(I_{Cerenkov}\right)}_{3}, \quad (1)$$

where r is the fibre core radius, α is the angle between the axis of the fibre and particle direction of travel, v is the speed of the particle, n is the fibre core refractive index, Δn is the

refractive index between the core and the fibre cladding and c is the speed of light. It can be split into three main components labelled here as Part 1–3.

Part 1 describes the path of the particle through the fibre with respect to the core of the fibre. Part 2 gives the fraction of the Cerenkov cone guided by the fibre, and Part 3 is the total intensity of Cerenkov radiation generated per unit distance. Thus Part 1 and 3 give the total intensity of Cerenkov generated by a charged particle passing through the optical fibre. The geometry of the Cerenkov cone and its coupling to a fibre is shown in *Figure* ***2***.

For the fibre used in NanoSpec a single particle generates very few photons (order 100s), so a single event will have no impact on the device performance. When the orbit passes through the magnetic poles and the SAA the cumulative effect of many events in single exposure could result in a detectable signal, however this assumes the detector is somehow unaffected by the increased radiation.

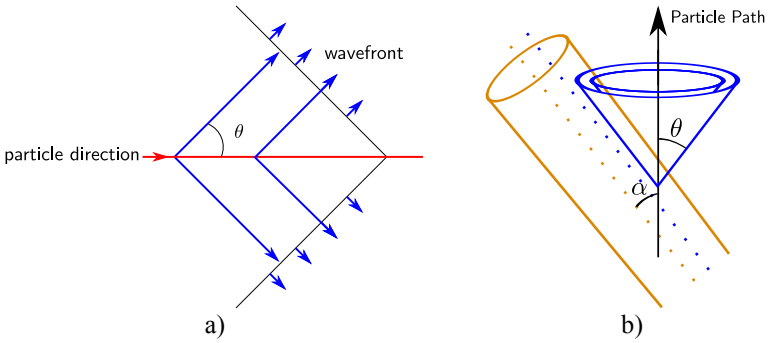

Figure 2: a) A plane wavefront of Cerenkov radiation is formed at an angle θ to the velocity of the particle. b) Only the portion of the Cerenkov cone that intersects with the fibre core and is within in the critical angle of the fibre is trapped. Illustrated is the case where the cone is parallel to the fibre, which maximises the fraction of the cone trapped [14]

NanoSpec

The goal of NanoSpec is to demonstrate the potential of photonics-driven technology in space-based applications. To that end we have designed and built a photonic spectrograph, specifically a single mode fibre-fed diffraction limited device, which will survive a launch into space while still providing a reasonable spectral resolution. The spectrograph design is based upon the relatively simple PIMMS#0[3] type device discussed by Bland-Hawthorn *el al.* in Ref. [15]. In contrast to most conventional spectrographs, the PIMMS spectrograph design is effectively independent of its light source (i.e. a telescope). This is because multiple single mode fibres feed the spectrograph. The key advantage here is that single mode fibre inputs are by definition diffraction limited. This essentially means the light in a single mode fibre is guided in the smallest area possible. This fundamental propagation mode always has a Gaussian profile, independent of the original light that was coupled into the fibre [16]. The result is multiple single mode fibres arranged side-by-side to form a diffraction-limited pseudo slit.

The single mode fibre feed can be linked to essentially any light source via an invention, called the photonic lantern. The photonic lantern efficiently converts light in a single multimode fibre (which is easily coupled to a variety of light sources) to multiple single-mode

[3] Photonic integrated multimode micro-spectrograph

fibres [17, 18]. This allows for a simpler spectrograph design, without sacrificing spectral resolving power, resulting in a compact and low cost device. It also reduces complexities in alignment and construction (specifically maintaining optical alignment during and after a launch into orbit) by reducing the number of components required.

NanoSpec is designed to be compatible with a photonic lantern input, however it has not yet been determined if the final flight instrument will utilize one (the current generation of lanterns are to large). The alternative is to form the pseudo slit in NanoSpec with 8 independent single mode fibres. They are to be arranged in pairs and point in four different directions out the sides of the TubeSat, as illustrated by the red and blue lines in Fig. 3b. This arrangement is intended to maximise the chances that the orientation of the spacecraft will allow spectra to be observed of the Earth, Sun, Moon or other astronomical sources (or a combination of these). The fibres have a numerical aperture of 0.1 (acceptance half angle of 5.75 degrees) corresponding to circular area with a radius of ~30km when the fibre is aimed at the earth surface. Additionally, the fibre pairs consist of two different types of fibre (discussed in the optical design section) in order to test their performance in the LEO environment.

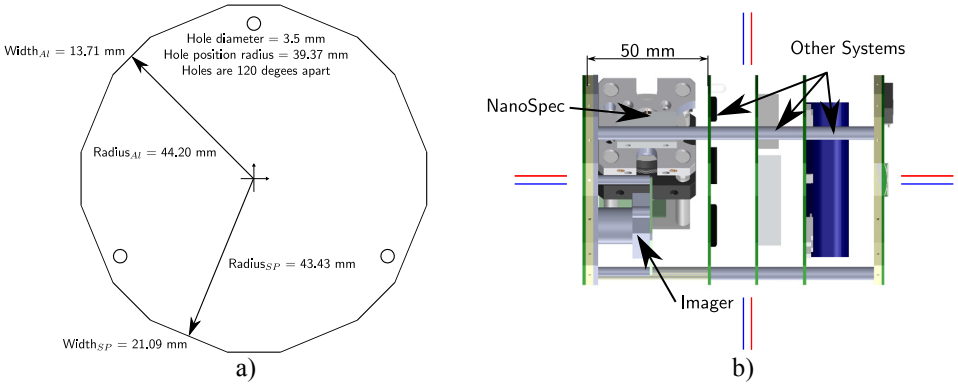

Figure 3: a) Diagram showing the dimensions of a blank PCB used in the TubeSat. The NanoSpec housing must fit within this area to be compatible with the TubeSat design. b) Side view schematic of the TubeSat. The payloads, including NanoSpec, are located in the leftmost compartment, with the other satellite systems composing the remaining space (Note – the radiation counter is obscured in the diagram).

Design Considerations

The primary constraints, and thus design drivers for NanoSpec, can be split into 3 main categories. The first is the restricted area and volume of the TubeSat, and is perhaps the most stringent constraint. Fig. 3a is a diagram of the PCBs that form the floor areas of i-INSPIRE and hold the spacecraft systems and payload. The science payload (including all optics, detectors/sensors and any additional control electronics) must remain within this footprint. Additionally the payload compartment, seen in the bottom of Fig. 3b limits the cumulative height of the payloads to 50 mm.

The overall cost of the spectrograph is the second major factor. The i-INSPIRE mission is a one-way trip, so anything that is launched into orbit will not be recovered. In fact, given that we are scheduled on the first mission of IOS's N45 launch vehicle, there is a significant risk that the satellite will not achieve orbit. This lead to the decision to keep the payload costs as low as possible, making use of commercially available parts and components where possible. Further, due to the low altitude and the actual mission time being fairly short (<4 weeks), we have neglected radiation hardness requirements in many of our components, opting for an industrial version where possible.

The third requirement arises from the limited power available to the payload in orbit. As an isolated system in-orbit the power budget is strict, so the power requirements of the detector used in the spectrograph are an important part of its design.

In order to satisfy both the cost the size and cost constraints the spectrograph will operate in the visible (~400-750nm). The performance of 'off the shelf' achromatic lenses reduces this to a wavelength range 450- 700nm. A visible light design is further supported by the wide availability of silicon CCD and CMOS detectors thanks to mass commercialisation of the technology.

Optical Design

Input Fibre

The current implemented design has 8 single mode fibres set in a v-groove fibre array manufactured by OzOptics[4] forming the input slit for the spectrograph. The v-groove allows the fibre inputs of the spectrograph to be precisely aligned and held. The fibre cores are separated by 127μm, while the faces of the fibres are coplanar. The array of fibres is arranged parallel to the axis of the diffraction grating such that their dispersed images form 8 independent spectra.

There are two different types of optical fibre used in NanoSpec. One is a typical step index fibre where light guiding is achieved via a higher refractive index in the core of the fibre than the cladding. The second is a photonic crystal fibre (PCF) where light is guided by a pattern of air filled holes in the core of a silica fibre. To our knowledge this will be the first time the use of PCF has been demonstrated in a space environment. If NanoSpec does suffer from signal to noise ratio degradation due to Cerenkov light, we expect the PCF fibre to exhibit better performance as it has less high-index material for the charged particle to pass through.

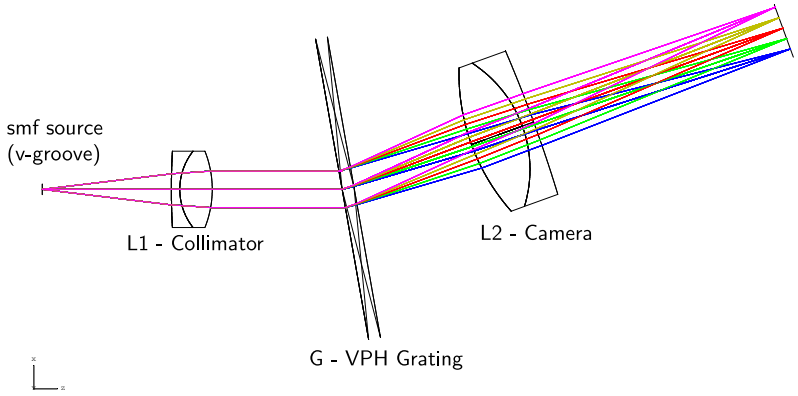

Figure 4: Diagram of the current layout for the NanoSpec micro-spectrograph. The v-groove array of input fibres are stacked perpendicular the page. Wavelengths are evenly spaced from 450 to 700 nm.

Collimator and Camera Optics

The collimator or collection system converts the f/5 (numerical aperture of 0.1) output beam from the single mode fibres to a collimated beam, which can be spectrally dispersed by a diffraction grating. After the beam has been dispersed it is then re-imaged onto the detector as

[4] http://www.ozoptics.com/

8 independent spectra. The collimating system in NanoSpec is composed of a carefully selected 'off the shelf' achromatic doublet lenses manufactured by the Newport Corporation[5] and Thorlabs[6]. The lenses are chosen to create the largest collimated beam (beam size is directly proportion to the resolution), yet remain diffraction limited and fit within the size constraints discussed previously. All lenses have an anti-reflective coating for visible light (400-700nm).

There are currently two versions of the collimator to suit two different detector pixel sizes (2.2μm and 6μm). The first is a doublet with an effective focal length (EFL) of 12.7mm. Resulting is a Gaussian beam approximately 2 mm in diameter (*d*; the diameter is measured at the points where the beam drops to $1/e^2$ of its peak intensity). The second version adds a second doublet with a 7mm EFL positioned 1mm in front of the first lens. This reduces the EFL of the collimator to 5.7mm and the beam width to 0.9 mm. The reduced beam size will also reduce the resolution of the spectrograph. The camera lens is a doublet with an EFL of 25.4mm in both cases. In all instances the optics are essentially very close to diffraction limited in the visible.

Grating

The dispersing element in the spectrograph is a volume phase holographic (VPH) grating manufactured by Wasatch Photonics[7]. It disperses the light from the collimator spectrally before it is re-imaged on to the detector. A VPH consists of a dichromate gelatine substrate with a controlled thickness between two pieces of protective glass with an anti-reflective coating. The VPH diffracts light via fringes of refractive index variation written in the gelatine substrate [19], rather than the physical lines/rules found in traditional gratings. This results in grating that is 'blazed' such that > 80% of diffracted light is transmitted in the 1st diffraction order (m = 1) over an extended wavelength range at angles, θ, consistent with the standard diffraction equation, $d\sin\theta = m\lambda$. Further, VPH gratings offer low scatter (which simplifies the design) and low wavefront distortion (necessary for a diffraction limited system).

In a spectrograph the number of combining beams generated at the diffraction grating gives a fundamental limit on the resolution. This corresponds to the number of lines on the grating that are illuminated by the collimated beam (N) and the diffraction order (m) as follows,

$$\mathrm{R} = \frac{\lambda}{\Delta\lambda} = \underbrace{mN}_{\text{uniform}}, \tag{2}$$

where $\Delta\lambda$ is the smallest spectral feature that can be resolved (often the full width at half maximum [FWHM] of the spectra line) and λ is the wavelength being measured. Note that Eqn. 2 assumes uniform illumination of the lines, whereas the beam in NanoSpec is Gaussian in nature. It can be shown that the resolution of the a Gaussian beam is given by the following,

$$R = \underbrace{2.38\tan\theta\frac{d}{\lambda}}_{\text{Gaussian}}, \tag{3}$$

where θ is the diffraction angle and *d* is the collimated beam width. At first glance it would appear that a Gaussian beam results in a higher resolution, however this is not the case as the

[5] http://www.newport.com/
[6] http://www.thorlabs.com/
[7] http://wasatchphotonics.com/

diameter in Eqn. 3 is only the $1/e^2$ width (i.e. a 1 mm Gaussian beam illuminates more grating lines than a 1mm uniform beam, albeit unevenly).

Detector

There are two detectors used in NanoSpec, one is used for ground testing and observation and the other will be used in flight. The first is 5MP (2552 x 1964) detector with 2.2μm pixels while the second is of the smaller VGA (640x480) format with 6μm pixels. The advantages of the VGA detector vs. the 5MP detector are a simpler TTL level serial interface and higher sensitivity. However due to the increased pixel size it must be paired with the shorter focal length collimator discussed previously. As a result the spectral resolution and range are unsurprisingly reduced. The 5MP detector has a USB interface, and allows greater control over pixel binning and exposure times. This allows for a more detailed study of NanoSpec's optical performance in the laboratory.

Preliminary results

Figure 5 is a spectrum from NanoSpec (using the 2.2μm detector) of the low-pressure gas discharge lines of mercury and argon generated by a Hg-1 calibration source manufactured by OceanOptics[8]. We have used this to calibrate the wavelength scale and probe the resolution of NanoSpec. The inset in Fig. 5 is an expanded view of the first order mercury (Hg-I) spectral lines at 576.96 and 579.06nm. From these we have determined the resolution, using Eqn. 2, where $\Delta\lambda$ is the FWHM of the line. Measurements of both lines result in a resolving power on the order of ~1400 ($\Delta\lambda \approx 0.4$nm). The theoretical resolution given by Eqn. 3 for these wavelengths is ~1450. Note that when the 6μm detector is used, we expect the resolution to be roughly half (due to the decreased beam size). This is extremely promising as it demonstrates that the device is diffraction-limited. Finally, initial measurements indicate that the throughput of the spectrograph is ~70%, where the primary loss of light is in unused diffraction orders of the VPH.

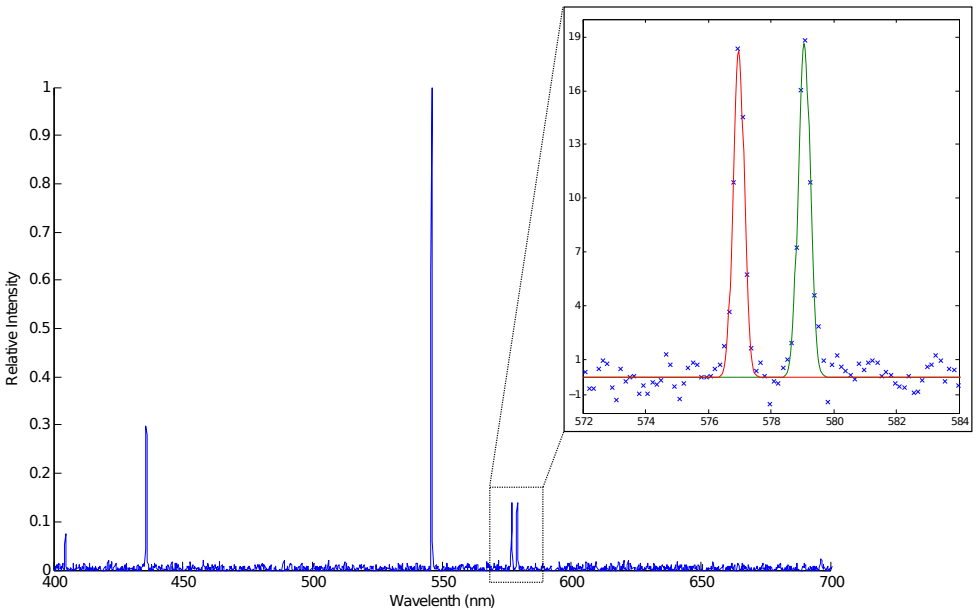

Figure 5: Example spectrum from NanoSpec of low-pressure gas discharge lines of mercury and argon captured using the 2.2μm pixel detector. Inset: Zoom in of the spectral lines at 576.96 and 579.06nm fitted with Gaussian profiles to determine the FWHM.

[8] http://www.oceanoptics.com/

Imaging camera

The third instrument on i-INSPIRE is an imaging camera designed and built by LinkSprite for the hobbyist community. It was chosen for two reasons: firstly it is controlled over a TTL level serial interface allowing simple integration with the i-INPSIRE micro-controller; secondly it has built in JPEG compression allowing higher resolution images in the available data budget. The primary goal of the imager is to obtain images of the Earth from orbit (for PR use). We also believe that a series of images taken at regular intervals will allow us to determine an approximate attitude of the spacecraft, in case of inertial measurement unit (IMU; [2]) failure. As i-INSPIRE does not have any attitude control, we cannot control where it is pointing while in orbit. The imager will take images at regular intervals (that are out of phase with the predicted pitch of the tumble) to ensure that an image of the Earth is taken. There are two options for the orientation of the camera in the TubeSat, the first is pointing out through a hole in one of the wall segments and the second is to point through the PCB floor. The optimal position of the camera in the TubeSat has not been determined yet as the expected profile of the TubeSat's movement in orbit is still under investigation.

Future Plans

The next step beyond i-INSPIRE will likely be a larger payload on a balloon-based platform. A balloon-based instrument will allow us to use scientific grade detectors (which have a larger footprint) to construct a more sensitive NanoSpec. Paralleling that, we hope to move toward a fully photonic device, likely using an arrayed waveguide grating. The first steps towards such a device was recently been demonstrated by Ref [20].

Conclusion

Here we have presented the planned instrumentation of the i-INSPIRE satellite. The primary instrument is the diffraction-limited micro-spectrograph dubbed NanoSpec, which has a measured resolution of 1400 (~0.4nm) @ ~578nm. With this we will demonstrate diffraction limited spectrograph in space and study the effects of the LEO radiation environment. With the on-board radiation counter we will generate a map of the radiation environment in LEO and correlate this with signals in NanoSpec data. Finally, with our on-board imager, we will obtain the first images of Australia from an Australian university satellite.

References

1. L. Fogarty, I. Cairns, J. Bland-Hawthorn, X. Wu, C. Betters, J. Funamoto, S. G. Leon-Saval, T. Monger*, et al.*, "The initial-INtegrated SPectrograph, Imager and Radiation Explorer (i-INSPIRE) - a university satellite project.," presented at the Proceeding of the 11th Australian Space Science Conference, 2011.
2. S. Xiao, X. Wu, I. Cairns, J. Bland-Hawthorn, C. Betters, J. Funamoto, S. G. Leon-Saval, L. Fogarty*, et al.*, "i-INSPIRE Tube-Satellite Bus Design," presented at the Proceeding of the 11th Australian Space Science Conference, 2011.
3. E. R. Benton and E. V. Benton, "Space radiation dosimetry in low-Earth orbit and beyond," *Nuclear Instruments and Methods in Physics Research B,* vol. 184, pp. 255--294, sep 2001.
4. D. M. Sawyer and J. I. Vette, "AP-8 trapped proton environment for solar maximum and solar minimum," *NASA STI/Recon Technical Report N,* vol. 771, p. 18983, December 1976.

5. D. Heynderickx, B. Quaghebeur, J. Wera, E. J. Daly, and H. D. R. Evans, "New radiation environment and effects models in ESA's space environment information system (SPENVIS)," presented at the Proceedings of the 7th European Conference on Radiation and Its Effects on Components and Systems, 2003. RADECS 2003., 2003.
6. M. Kruglanski, E. de Donder, N. Messios, E. Gamby, L. Hetey, S. Calders, and H. Evans, "SPENVIS - Space Environment, Effects, and Education System," *spenvis.oma.be,* 2011.
7. A. J. Tylka, J. H. Adams Jr, P. R. Boberg, B. Brownstein, W. F. Dietrich, E. O. Flueckiger, E. L. Petersen, M. A. Shea*, et al.*, "CREME96: A Revision of the Cosmic Ray Effects on Micro-Electronics Code," *Nuclear Science, IEEE Transactions on,* vol. 44, pp. 2150--2160, 1997.
8. D. Biesecker and the Solar Cycle 24 Prediction Panel, "Solar Cycle Progression and Prediction," *url*http://www.swpc.noaa.gov/SolarCycle/, May 2009.
9. G. D. Badhwar, "The radiation environment in low-Earth orbit," *Radiation research,* vol. 148, pp. S3--S10, nov 1997.
10. J. Abraham, M. Aglietta, I. C. Aguirre, M. Albrow, D. Allard, I. Allekotte, P. Allison, J. A. MuÃ$\pm$iz*, et al.*, "Properties and performance of the prototype instrument for the Pierre Auger Observatory," *Nuclear Instruments and Methods in Physics Research Section A: Accelerators, Spectrometers, Detectors and Associated Equipment,* vol. 523, pp. 50 - 95, 2004.
11. Y. Fukuda, T. Hayakawa, E. Ichihara, K. Inoue, K. Ishihara, H. Ishino, Y. Itow, T. Kajita*, et al.*, "Measurement of a small atmospheric ν_μ / ν_e ratio," *Physics Letters B,* vol. 433, pp. 9 - 18, 1998.
12. J. Lambert, Y. Yin, D. R. McKenzie, S. Law, and N. Suchowerska, "Cerenkov light spectrum in an optical fiber exposed to a photon or electron radiation therapy beam," *Applied Optics,* vol. 48, pp. 3362--3367, jun 2009.
13. S. H. Law, N. Suchowerska, D. R. McKenzie, S. C. Fleming, and T. Lin, "Transmission of Čerenkov radiation in optical fibers," *Optics Letters,* vol. 32, pp. 1205--1207, may 2007.
14. S. H. Law, S. C. Fleming, N. Suchowerska, and D. R. McKenzie, "Optical fiber design and the trapping of Cerenkov radiation," *Applied Optics,* vol. 45, pp. 9151--9159, dec 2006.
15. J. Bland-Hawthorn, J. Lawrence, G. Robertson, S. Campbell, B. Pope, C. Betters, S. Leon-Saval, T. Birks*, et al.*, "PIMMS: photonic integrated multimode microspectrograph," *Proc. SPIE,* vol. 7735, p. 77350N, 2010.
16. R. Paschotta, *Encyclopedia of Laser Physics and Technology*: John Wiley & Sons, 2008.
17. D. Noordegraaf, P. M. W. Skovgaard, M. D. Nielsen, and J. Bland-Hawthorn, "Efficient multi-mode to single-mode coupling in a photonic lantern," *Optics Express,* vol. 17, pp. 1988--1994, jan 2009.
18. S. G. Leon-Saval, A. Argyros, and J. Bland-Hawthorn, "Photonic lanterns: a study of light propagation in multimode to single-mode converters," *Optics Express,* vol. 18, p. 8430, apr 2010.
19. S. C. Barden, J. A. Arns, W. S. Colburn, J. B. Williams, S. C. Barden, J. A. Arns, W. S. Colburn, and J. B. Williams, "Volume−Phase Holographic Gratings and the Efficiency of Three Simple Volume−Phase Holographic Gratings," http://dx.doi.org/10.1086/316576, vol. 112, pp. 809--820, jun 2000.
20. N. Cvetojevic, N. Jovanovic, J. Lawrence, M. Withford, and J. Bland-Hawthorn, "Developing arrayed waveguide grating spectrographs for multi-object astronomical spectroscopy," *Opt. Express,* vol. 20, pp. 2062-2072, 2012.

i-INSPIRE Tube-Satellite Bus Design

Size Xiao[1], Xiaofeng Wu[1], Iver Cairns[2], Joss Bland-Hawthorn[2], Chris Betters[2], Jiro Funamoto[1], Sergio Leon-Saval[2], Lisa Fogarty[2], Tony Monger[2], Xueliang Bai[1]

[1] School of Aerospace, Mechanical and Mechatronic Engineering, University of Sydney, NSW, Australia, 2006
[2]School of Physics, A28, University of Sydney, NSW, Australia, 2006

Summary: i-INSPIRE (initial - INtegrated SPectrograph, Imager and Radiation Explorer) is a collaborative project between the School of Aerospace, Mechanical and Mechatronic Engineering and the School of Physics within the University of Sydney. The project aims to verify the ability of a 1 kg pico-satellite to carry advanced space and astronomical payloads (a radiation counter, photonic spectrograph, and a CMOS [Complementary Metal Oxide Semiconductor] imager). As the first pico-Sat to be fully constructed by one Australian university and to be launched into space, the i-INSPIRE project will be a prototype for future larger and more complex nano-satellite platforms. The satellite platform distributes the power, communication and control subsystems into three individual PCBs (Printed Circuit Board). Observational data from payloads will be collected and stored in an external memory device, which is connected to the micro-controller by an SPI (Serial Peripheral Interface) interface. A FM transceiver, the main part of the communication subsystem, will work in the UHF (Ultrahigh Frequency) band and initially be in beacon mode. After obtaining a confirmation signal from the ground station, the microcontroller will transmit house-keeping and payload data to the ground station at the University of Sydney. The addition of a nano-IMU (Inertial Measurement Unit) is being considered to determine the current attitude of i-INSPIRE, in order to complement and confirm the pointing inferred from the imaging camera.

Keywords: TubeSat, On-Board Data Handling (OBDH), systems, UHF communication

I. Introduction

The primary objective of the i-INSPIRE project is to conduct multiple scientific observations. As a secondary objective, new pico-satellite technologies for future projects will be demonstrated. The satellite body is cylindrical with a 9 cm diameter and 13 cm height. Since it has a tubular shape, this satellite is called a TubeSat. Including payloads, the expected full weight can be less than 1 Kg. F*ig.1* shows the overall bus design of the TubeSat. The launch is planned for March-July in 2012. A polar, circular orbit near 310 km has been selected. For on board data processing, a radiation counter, a photonic spectrograph, a CMOS imager and other components are wired to a BX-24 controller which is integrated on OBDH board. The UART (Universal Asynchronous Receiver Transmitter) and SPI bus provided on the controller are efficiently used for realizing data transfer. For downlink and uplink communication, data will conform to the AX.25 protocol and transmitted via the FSK (Frequency-Shift Keying) modulation.

II. Satellite bus

The mechanical structure of the TubeSat consists of five PCBs that are enclosed into an aluminium frame, as shown in *Fig. 1*. A pair of dipole antenna are soldered on the top board and physics payloads are located on the bottom layer within the TubeSat. In the middle of the frame, power management, communication, and OBDH subsystems are distributed onto the three remaining PCBs [6]. Tiny ribbon-cables will be used for all connections among boards. As the core of the whole system, the OBDH board will control the peripheral components while storing and retrieving data. In addition, one low power consumption IMU may be added to provide satellite body attitude information which could be meaningful for the scientific observation payloads.

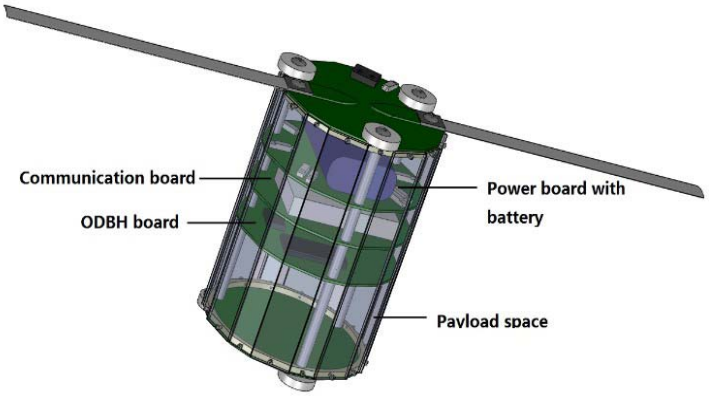

Fig. 1: TubeSat structure

A. Power management subsystem

The Power Management (PM) subsystem consists of two parts, the solar panels and power management components. Solar panels are designed to convert solar energy to electrical energy, with a typical output of 2.52V per panel. The voltage is raised by a current sense amplifier to 4.2V for charging the battery. Solar cells are attached to alternating long vertical strips of the external surface of the TubeSat. All power management components are integrated into one PCB. This Power Management board provides power to other subsystems and also includes infrastructure for measuring the voltage delivered by the cells.

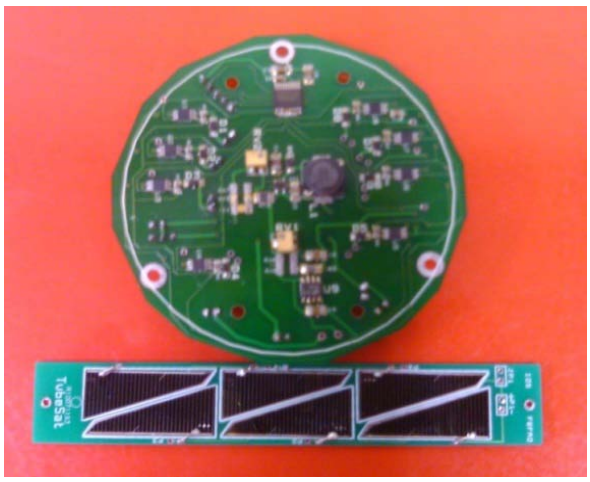

Fig. 2: PM PCB with solar cells

Basically, the PM function is designed to connect the solar panel and the lithium-ion battery, and to monitor the status of each solar panel. All the voltages needed by other subsystems are converted by the PM board. The output voltage from solar cells will be regulated for two times. A typical low dropout voltage (LDO) linear regulator and boost voltage converter are used in the PM system. Original voltage from parallel solar cells will pass through the LDO regulator and converted to 4.2V, which is the voltage for battery recharging. And then, boost voltage converter will step up the power to 5.7V to feed other subsystems. The power consumption details of TubeSat are listed in *Fig. 3.*

Power budget			
Subsystem	**Power(mW)**	**Duty cycle(hrs/day)**	**mWh/day**
Power	1000	19.4	19,400
Onboard data handling	250	24	-3000
Communication	27~500	13	-2459
Payloads			
Total Energy Available (mWh): 9620 **Total Used (mWh):8100** **Energy remaining (mWh)：1520**			

Fig. 3: Power management structure

In particular, current-sense amplifiers and one 8-bit SPI interface AD convertor make up the monitor. A current-sense amplifier is a special purpose amplifier that output a voltage proportional [3] to the current flowing in a power trail. It utilizes a "current-sense resistor" to convert the load current in the power trail to a small voltage, which is then amplified by the current-sense amplifier. Voltage level data will be transferred to the BX-24 controller via AD convertor. It is worthwhile to point that the voltage level can roughly indicate Sun's light intensity since the output voltage of solar panel is directly proportional to light intensity until saturation.

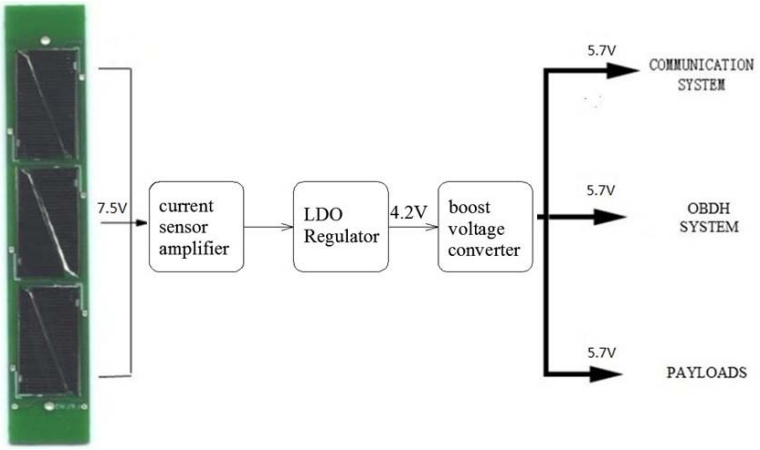

Fig. 4: Power management structure

B. On-Board data handling (OBDH) subsystem

The TubeSat uses a BX-24 module as the central controller. The BX-24 Microcontroller is

based on an AVR single-chip [4], and is an integration of the Atmel AT90S8535 and its application circuit. The BX-24 has 16 general purpose I/O (Input / Output) lines that are TTL (Transistor Transistor Logic) and one SPI interface. When used for digital I/O, each line can be set to one of four states -- output high, output low, input tri-state (hi-Z) and input with pull-up resistor. Meanwhile, one PIC16F627 controller is integrated onto the OBDH board uplink communications.

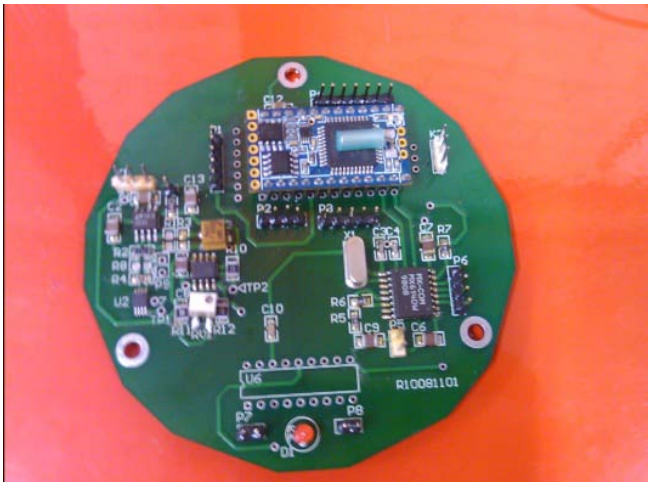

Fig. 5: ODBH PCB

Each proposed payload and the communication subsystem will occupy a pair of general I/O ports for Transmitting/Receiving. The spare I/O ports can be used as handshake lines for the data transfer. *Fig. 6* shows how the BX-24 connects to the other subsystems.

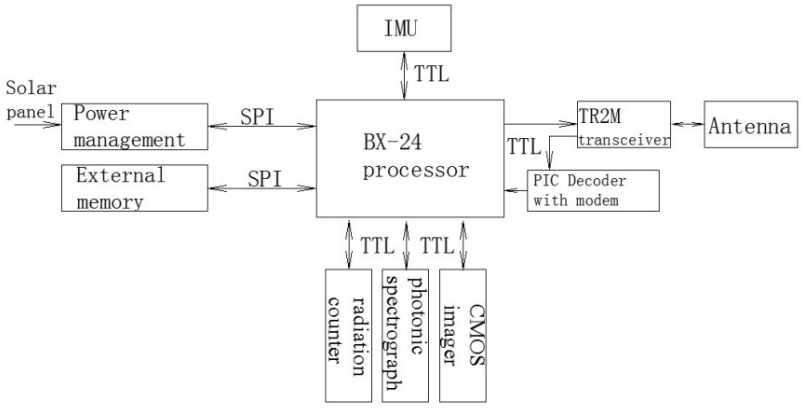

Fig. 6: Data bus of TubeSat

The behavior of the OBDH subsystem is governed by a simple state machine and the relevant program code is written in the Basic language. In this state machine, as shown in *Fig. 7*, all states are in a loop. After successful initialization, the controller will start collecting observation data from payloads, then establish the link with ground station and complete data transmission.

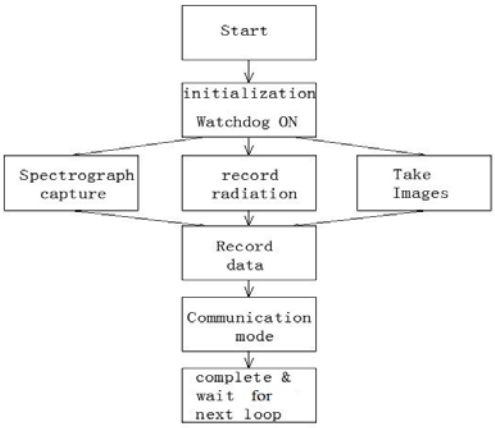

Fig. 7: States of processor operations

C. Communication subsystem

This system is for transmitting and receiving the signals and so must be able to switch from transmitter mode to receiver mode. So the transceiver is designed to select a different frequency according to three address pins. In order to ensure the power of the transmitting signal is large enough to be received on Earth, an amplifier is used to increase the power of the signal.

The current design uses a TR2M transceiver, which works in the frequency range of 433-434 MHz, at a power of 100 mW [5]. A 500mW RF amplifier AFS2 is used to extend the operating range.

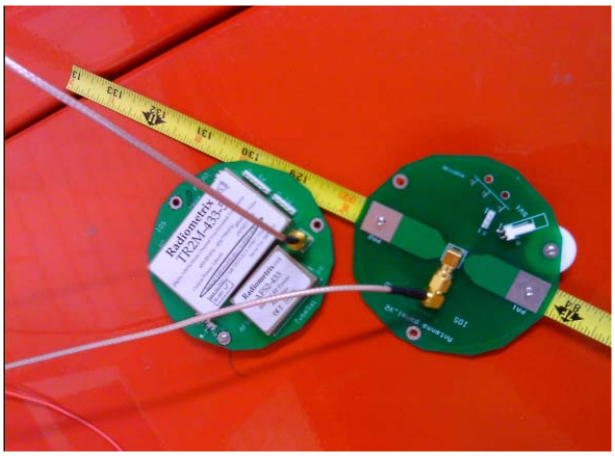

Fig. 8: TR2M transceiver (including AFS2 amplifier) with antenna

In order to obtain efficient data link, all the data in the uplink and downlink will be encoded into AX.25 protocol packets and then transmitted with FSK modulation at a 1200 baud rate [1]. Therefore, during the transmission mode, the BX-24 will work as the data packet encoder. In receiving mode, the independent PIC controller together with one FSK modem chip MX614dw is responsible for packet decoding and will deliver decoded instructions to the BX-24 controller.

The communication subsystem will work as one state machine as well. It is described in

Fig.9. When the satellite's main program enters communication mode, Morse or AX.25 beacons will be transmitted at fixed intervals while the satellite is waiting for the ground station's response. When the response is confirmed, the TubeSat will transmit data via the transceiver in AX.25 packet format. At the end, after sending all data, communication mode will be terminated and then the system will return to main program.

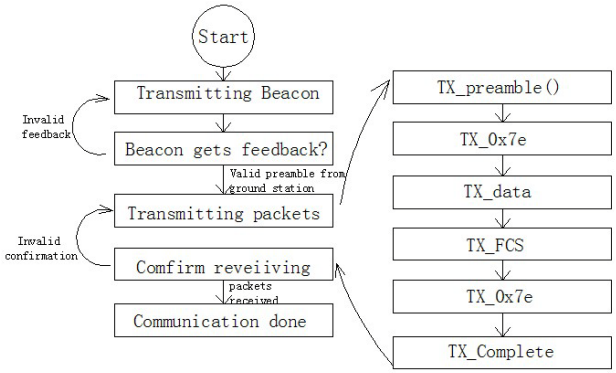

Fig.9 Flowchart of communication

III.PAYLOADS AND STORAGE

As mentioned above, the TubeSat carries three devices: a radiation counter, photonic spectrograph, and a CMOS imager. All of these are placed into one PCB at the bottom of the TubeSat. Hence, the attitude of the TubeSat will affect the observational results, especially for the CMOS imager. Under power conditions permits, an IMU could be useful for determining the best times to collect data.

The BX-24 controller will collect observational data from the three observation payloads and store them in order into an SD card through the SPI interface. When the satellite enters transmitting mode, the BX-24 will address the payload data in memory space and transfer them to the send buffer for transmitting.

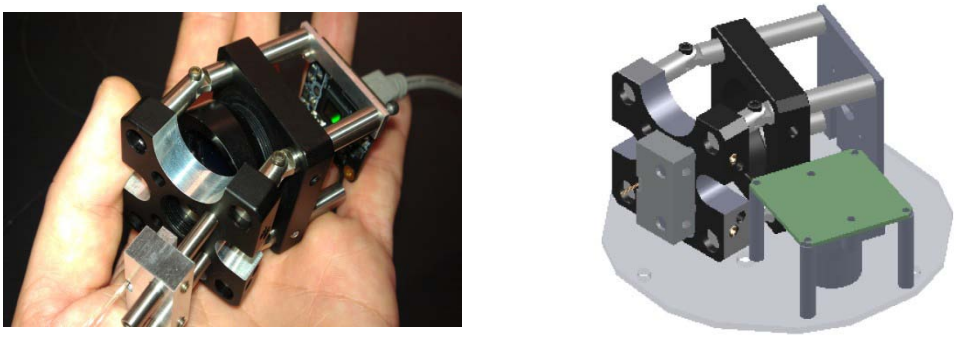

Fig.10 photonic spectrograph and proposed payloads model [2]

CONCLUSION

This paper demonstrates the detailed bus design for the i-Inspire project. The distributed subsystems leave more space for partial upgrade in the future. Based on UART and an SPI interface, all subsystems are controlled by the main controller on the OBDH board and

extended storage device is applied to increase memory space. The AX.25 protocol is adopted in the UHF band communication to decrease the error rate and improve efficiency. IMU is considered to assist payloads in getting ideal data. This design shows a reliable platform for the payloads and fully employs the on-board hardware resources.

References

[1] Larson, W.J., Wertz, J.R., "Space Mission Analysis and Design," 3rd ed., Microcosm, El Segundo, 1998, pp. 381-394.

[2] C. Betters, I. Cairns, J. Bland-Hawthorn, X. Wu, L. Fogarty, J. Funamoto, S. G. Leon-Saval, T. Monger, and S. Xiao, "Instrumentation of the i-INSPIRE satellite," in Proceedings of the 11th Australian Space Science Conference, 2011.

[3] MAX9928/MAX9929, -0.1V to +28V Input Range to +28V Input Range, Micro-power, Uni-/Bidirectional, Current-Sense Amplifiers, http://datasheets.maxim-ic.com/en/ds/MAX9928F-MAX9929F.pdf

[4] BX-24 Hardware Reference, http://www.basicx.com

[5] Radiometrix Narrow Band FM Multi-channel UHF Transceiver TR2M-433-5, http://www.radiometrix.com/content/tr2i-tr2m

[6] TubeSat Personal Satellite Kit Assembly Guide, http://www.interorbital.com

Engineering i-INSPIRE - a Pico-Satellite from Australia

Jiro Funamoto*†, Xiaofeng Wu*, Iver H. Cairns†, Joss Bland-Hawthorn†, Chris Betters†, Lisa Fogarty†, Sergio G. Leon-Saval†, Anthony G. Monger† and Size Xiao*

* *School of Aerospace, Mechanical and Mechatronic Engineering, The University of Sydney, NSW, 2006, Australia*
† *School of Physics, The University of Sydney, NSW, 2006, Australia*

Summary: This paper provides details on the design, testing, launch, orbital characteristics, and operation of i-INSPIRE (the initial - INtegrated SPectrograph, Imager and Radiation Explorer), a tube-shaped pico-satellite currently being developed at the University of Sydney for an anticipated launch in 2012. i-INSPIRE is aimed to be the first pico-satellite to be designed, built and operated in space by a single Australian university and is expected to return the first spectra from a novel spaceborne photonics-based spectrograph, radiation maps of the Earth at an altitude of 310 km, and the first images of Australia from an Australian satellite. This paper complements a set of other papers about i-INSPIRE, those being (1) the overview (Fogarty et al. [1]), (2) the onboard instruments (Betters et al. [2]), and (3) detailed characterisation of the satellite subsystems and protocols (Xiao et al. [3]).

Keywords: satellite, pico, Australia, university, spectrograph, photonic, radiation, camera

I. Introduction

i-INSPIRE, the initial - INtegrated SPectrograph, Imager and Radiation Explore (Fig. 1), is a tube-shaped pico-satellite[1] currently being developed at the University of Sydney for an anticipated launch in 2012. i-INSPIRE carries three instruments, (1) a novel photonics-based miniature spectrograph “NanoSpec”, (2) a radiation counter, and (3) an imaging camera.

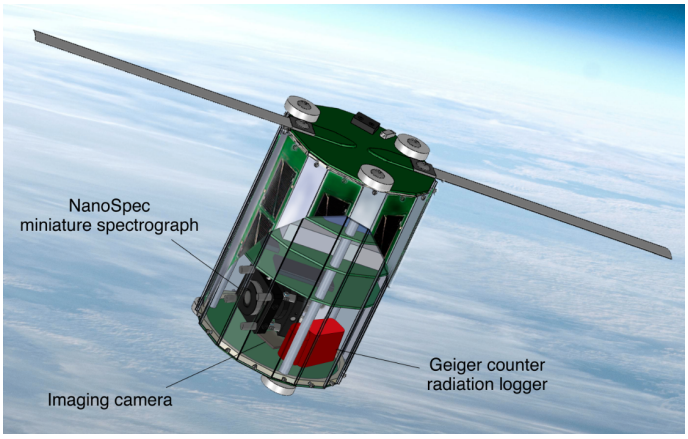

Fig. 1: A simulated, cut-away image of the i-INSPIRE satellite in orbit

[1]By definition pico-satellites have masses from 0.1 to 1 kg. Other classifications include nano-satellites with masses from 1 to 10kg, and micro-satellites with masses from 10 to 100kg.

i-INSPIRE is a joint project between the University's School of Aerospace, Mechanical and Mechatronic Engineering and the School of Physics. It aims to be the first pico-satellite to be designed, built and operated in space by a single Australian university.

The goals of i-INSPIRE are both technological and scientific. Detailed goals can be found in Fogarty et al. [1]. Briefly, the technological goals include the successful design, construction, launch and operation of i-INSPIRE. Scientific goals include the first ever tests of a photonics-based miniature spectrograph (see Betters et al. [2]) in space, and the correlation between Cerenkov light generated in the spectrograph optical fibres and the local radiation level measured by a separate radiation counter.

i-INSPIRE is envisioned to be an initial, smaller test satellite for a larger future satellite, INSPIRE. Where i-INSPIRE is a testing platform and technology demonstrator, INSPIRE is intended to be a more scientifically capable satellite that will perform cutting edge science. i-INSPIRE is therefore an important precursor of possible larger Australian satellites to come.

The following sections of this paper will describe various engineering-specific aspects, including the design, testing, launch, orbital characteristics and operation of i-INSPIRE.

II. Design of i-INSPIRE

The basic design of i-INSPIRE was provided by the launch company Interorbital Systems (IOS) as part of a pico-satellite launch package [4]. The three scientific instruments needed to be integrated into this basic design.

Exterior physical characteristics

i-INSPIRE is a 0.75kg tube-shaped (specifically a hexadecagonal prism) pico-satellite with a height and diameter of approximately 130 mm and 90 mm respectively (Fig. 2). i-INSPIRE is similar in volume and mass to the successful mainstream 'CubeSat' series satellites, but of different shape.

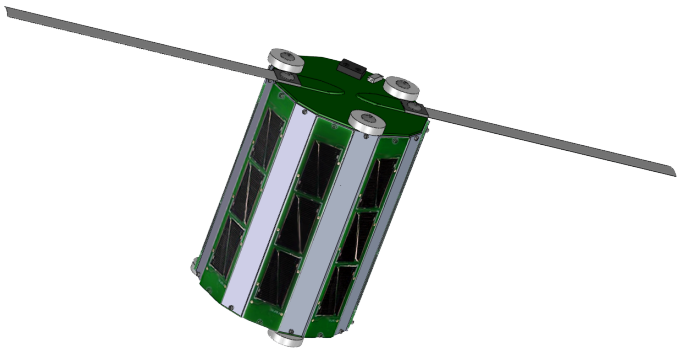

Fig. 2: Exterior view of the i-INSPIRE satellite. The exterior of the satellite is covered by alternating vertical aluminium strips and solar panels. The two elements of the antenna are secured to the top of the satellite, with a tip-to-tip length of approximately 330 mm.

The vertical hexadecagonal faces of the satellite alternate between solar panels and aluminium strips, with the former providing energy to recharge the onboard battery and the latter providing structural integrity necessary to withstand the g-loads and vibrations during launch.

The three small, white cylinders on each end of the satellite are bearings made of teflon which help to slide i-INSPIRE out of its ejection tube (on the launch vehicle) into space. Ejection is achieved by spring-driven ejection. The two elements of the centre-fed half-wave dipole antenna on the top of i-INSPIRE are made from spring steel, allowing them to be bent when packing i-INSPIRE in the ejection tube (Fig. 3).

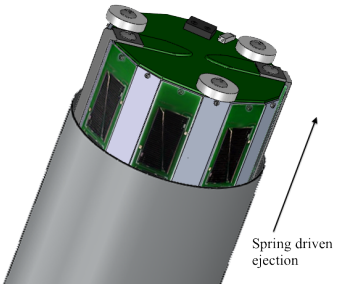

Fig. 3: Packing of i-INSPIRE inside the ejection tube. Antenna elements are made from spring steel and are bent inside the tube when i-INSPIRE is in the launch vehicle.

Interior physical characteristics

Fig. 4 shows the i-INSPIRE satellite without its aluminium strips and solar panels. The interior of the satellite is separated into several compartments, divided by printed circuit boards (PCBs) which hold electronic components and circuitry. Each PCB has a specific role in the operation of the satellite. The PCBs from the top to the bottom of the satellite are:

- antenna PCB (receives signals from and transmits signals to the ground station)
- power management PCB (regulates power to the satellite from the solar panels)
- transceiver PCB (decodes/encodes signals from/to the antenna)
- micro-controller PCB (controls the instruments onboard, and processes and stores data)
- experimental PCB (contains the electronic circuitry for the onboard scientific instruments)

These PCBs together perform everything i-INSPIRE needs to do, including collecting data from the onboard instruments, storing data in memory, establishing communication with an antenna on Earth (the ground station) and transmitting the data down to the ground station.

In Fig. 4, the lowest compartment of the i-INSPIRE satellite is empty. However, this compartment will contain the scientific instruments of the i-INSPIRE satellite:

- a miniature spectrograph (Fig. 5A),
- a radiation counter (Fig. 5B), and
- an imaging camera (Fig. 5C).

A detailed description of the instruments can be found in Betters et al. [2] and Fogarty et al. [1], and is not repeated here.

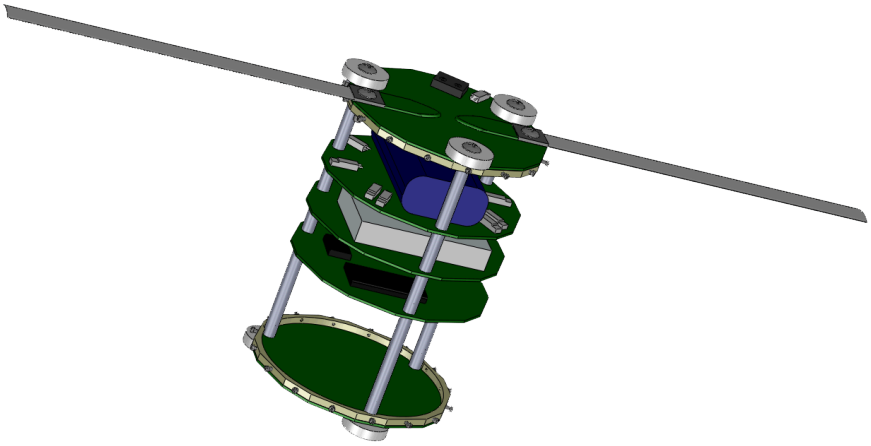

Fig. 4: Interior view of the i-INSPIRE satellite. The aluminium strips and solar panels have been removed, exposing the internal electronics and various compartments of the satellite. These compartments are separated by layers of electronic circuit boards (green).

A B C

Fig. 5: A) miniature spectrograph "NanoSpec", B) a radiation counter similar to the model being used, C) imaging camera. Images B and C from www.sparkfun.com. Pictures not in absolute or relative scale.

III. Testing

At the time of writing, comprehensive tests have not been performed on a fully integrated version of i-INSPIRE. The major tests to be performed are vacuum testing, radiation testing, vibration testing, and thermal testing. Three versions of i-INSPIRE will be built; an engineering model for testing, a flight model, and a flight spare. The flight model should be identical to the final engineering model, which will include modifications and revisions implemented as a result of the testing process. The basis of the tests and details of some testing facilities are now described.

Vacuum testing

Vacuum testing (simulating the vacuum environment of space) is necessary to verify that there are no unexpected structural or electronic failures caused by pressure differential (possibly by pockets of air trapped in components or compartments of the satellite) or outgassing. Any such failed components will be replaced or redesigned with vacuum-safe alternatives. Vacuum testing will be performed to a pressure of around 10^{-3} Pa, corresponding to about 10^{-8} atmospheric pressure. The vacuum chamber proposed to be used for this study is the bell chamber situated in the Fusion Studies Laboratory of the School of Physics at The University of Sydney, run by A/Prof. Joe Khachan.

Radiation testing

A significant level of radiation (a combination of high energy particles and electromagnetic radiation) exists at the operational altitude of 310 km for i-INSPIRE. To simulate the radiation damage to the satellite over a specified period (e.g. 1 month), the equivalent radiation dose will be applied to the satellite using controlled sources of radiation, and the actual damage monitored. This will be an important test for i-INSPIRE which uses off-the-shelf electronic components.

Vibration testing

i-INSPIRE will experience large vibrational loads during launch, due to launch vehicle acoustics, resonant modes, and engine vibrations [5]. If the components and electrical connections inside the satellite are not properly fixed in place, or the satellite structure is not robust enough, these vibrational loads at launch could critically damage i-INSPIRE before reaching space. A vibration testing machine (a "shaker") will be used with vibration frequency spectrum data for the launch vehicle to be used (see Section "Launch") provided by the launch company.

Thermal testing

In orbit, i-INSPIRE will periodically move in and out of the shadow of the Earth. As a result the temperature of parts of i-INSPIRE are expected to fluctuate between approximately -20 and +70 degrees Celsius. Such thermal cycling continually contracts and expands satellite hardware, damaging the satellite over many cycles. The most accurate thermal cycling tests are done in a vacuum environment to allow for radiative heat transfer as the only means of heating and cooling of the satellite (as in space). i-INSPIRE will be tested in an appropriate thermal vacuum chamber, such as the bell chamber in the School of Physics.

IV. Launch

Once i-INSPIRE is built and tested, a launch vehicle will take i-INSPIRE into orbit. The following section presents the details of the launch vehicle expected to transport and deploy i-INSPIRE into orbit.

Launch date, location, and company

The i-INSPIRE satellite is scheduled for launch in mid to late 2012. The launch company is a private United States of America aerospace company founded in 1996, called "Interorbital Systems" (IOS), based in Mojave, California.

Much of the testing of the launch vehicle has been performed at the Mojave Air and Space Port by IOS. However, the actual launch is expected to be from an offshore platform about 250 km off the coast of California. The launch will be operated under a United States (US) launch license. In addition, for the i-INSPIRE satellite a separate Overseas Launch Certificate from the Australian Government is also necessary and an application is currently in-preparation.

Launch vehicle

The launch vehicle expected to carry and deploy i-INSPIRE into orbit is IOS's Neptune 45 launch vehicle (Fig. 6).

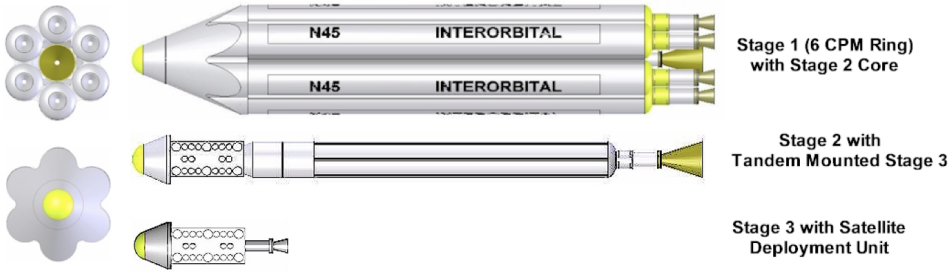

Fig. 6: The Neptune 45 launch vehicle developed by IOS. The Neptune 45 consists of 7 smaller rockets clustered together. The Neptune 45 can carry 45 kg to a polar Earth orbit of 310 km altitude. Image from [6].

The Neptune 45 has a modular rocket design, in which the complete launch vehicle is composed of a cluster of 7 smaller rockets (called "common propulsion modules" by IOS). Fig. 7 shows a common propulsion module rocket made for testing purposes.

As the launch vehicle ascends, different sets of common propulsion module rockets ignite and fall away after use (staging), a necessity to increase the efficiency of the launch vehicle. The Neptune 45 launch vehicle is a 3-stage launch vehicle (process shown in Fig. 8).

The Neptune 45 launch vehicle is capable of launching 45 kg into a polar Earth orbit at 310 km altitude. As a result, the Neptune 45 launch vehicle will launch a total of 32 tube satellites and 10 cube satellites, of which i-INSPIRE is one. The other groups launching these pico- and nano-satellites include various universities, high schools, and government entities from around the world.

Fig. 7: Common propulsion module rocket. Seven of these common propulsion module rockets and an additional booster stage compose the Neptune 45 launch vehicle. Image from [6].

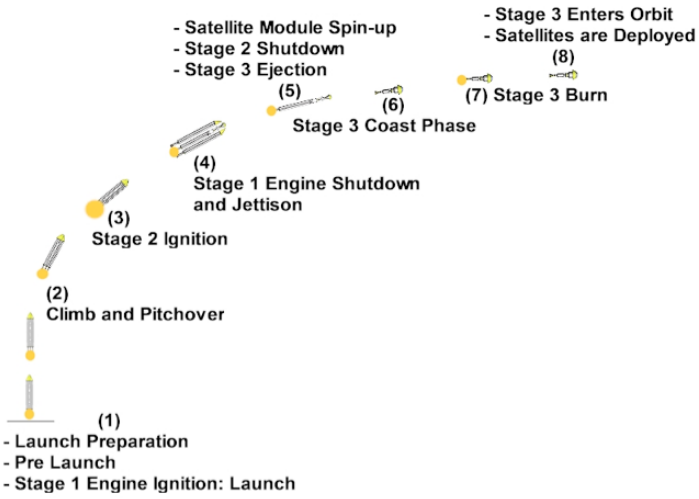

Fig. 8: The staging sequence of the Neptune 45 launch vehicle. In the 1st stage of launch, the outer 6 common propulsion modules ignite. After the 1st stage, the middle common propulsion module ignites to comprise the 2nd stage. The 2nd stage rocket then falls off to release the third and last stage which has a booster rocket to deliver the cargo (payload) into orbit. Image from [6].

V. Orbital characteristics and lifetime

Orbit

The Neptune 45 launch vehicle is expected to launch i-INSPIRE and other satellites into a 310 km altitude, circular, polar (inclination 90 degrees) Earth orbit. An orbit at 310 km has a period of approximately 90 minutes, resulting in roughly 16 orbits per day. A polar Earth

orbit is advantageous in this situation as the satellite will be able to see every region of Earth during one day[2]. This allows maximum coverage of the Earth such that any satellite operator will be able to 'see' their satellite at least once per day with a fixed ground station.

Lifetime

The lifetime of a satellite depends on numerous factors, with the most important being the atmospheric drag at the altitude of orbit. The predicted lifetime of i-INSPIRE is 24 days. This was calculated using the lifetime utility in the commercially available simulation software "Satellite Tool Kit" by Analytical Graphics, Inc. The predicted lifetime could be lower if unexpectedly high solar activity is present, as this expands the atmosphere, increasing drag at all orbital altitudes.

VI. Operation

Downlink of scientific data

To obtain scientific data collected aboard i-INSPIRE, the scientific data must be streamed from i-INSPIRE to a receiver on the ground (the ground station). For this downlink of scientific data, there must be (1) a transmitter on the satellite and a receiver on the ground station, (2) line of sight between the satellite and the ground station, and (3) a strong enough signal from the satellite to be detected by the ground station.

Constraint (1) is satisfied by the design of i-INSPIRE in Fig. 4 incorporating a transceiver (transmitter and receiver) system and by the existence of a dedicated ground station for i-INSPIRE at The University of Sydney. For the ground station, a tracking antenna has been mounted on the rooftop of the Electrical Engineering Building at The University of Sydney, specifically for the purpose of receiving data from i-INSPIRE. There is also a possibility to use international networks of ground stations to obtain a larger amount of scientific data per day though the downlink of data over different regions of the world. However, this has not yet been organised.

Constraint (2) is more difficult to satisfy (see Fig. 9). Since the satellite will be orbiting the Earth, there will be limited time when the ground station has direct line of sight access to the satellite. An orbital simulation using "Satellite Tool Kit" shows that as the satellite passes overhead, a ground station can see the satellite for an average of 7 minutes per sighting, and there will be 3 to 4 such sightings in one day. i-INSPIRE will be transmitting periodic beacon signals which notify the tracking station when the satellite comes into line-of-sight view. During each i-INSPIRE orbital passing, the ground station must track i-INSPIRE, and this is done by the automated tracking system on the ground station.

Constraint (3) is a further restriction to communication. Although the satellite is in view of the ground station, communication may not be possible if the signal strength from the satellite

[2]While the i-INSPIRE satellite orbits the Earth from North pole to South pole and back, the Earth continually spins beneath it, allowing the satellite to 'sweep' out continuously changing regions of the Earth and consequently the whole surface of the Earth in a single day.

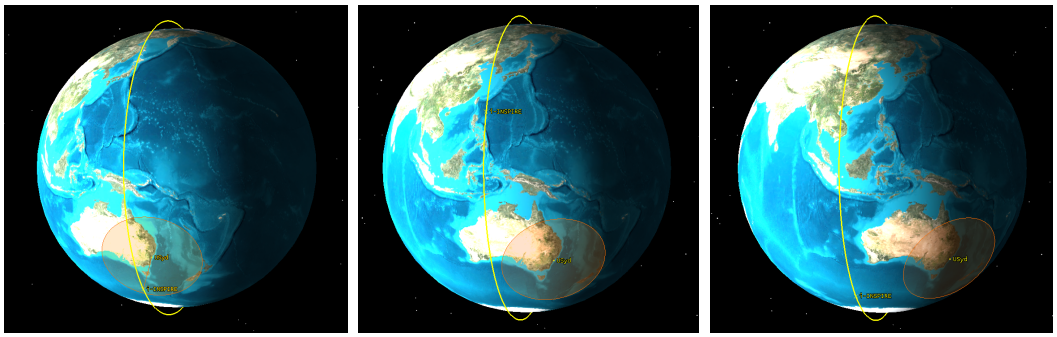

Fig. 9: i-INSPIRE can only communicate with the ground station when the satellite passes through the viewable/trackable disk of the ground station. As the satellite orbits the Earth, the satellite only spends on average 7 mins in this trackable disk of the ground station. Even though the satellite at 310 km altitude orbits the Earth approximately sixteen times in one day, since the Earth continually rotates beneath the orbit of the satellite, this results in only three to four such sightings of 7 mins each, over the course of a day. Images generated in Satellite Tool Kit, Analytical Graphics, Inc.

is too weak for the ground station to distinguish over electrical noise. A weak signal can be attributed to two major reasons: (i) signal attenuation due to too large a distance between i-INSPIRE and the ground station, and (ii) polarisation or antenna orientation mismatches. For communication analyses of this type, a useful calculation is that of the link margin (a value in dB expressing the further attenuation a signal can suffer before being unable to be detected by the ground station). For item (i) it is found that when i-INSPIRE is furthest away while still being in view (this happens when i-INSPIRE is just on the visible horizon), for a satellite transmission power of 0.5 W, the link margin is found to be approximately 6 dB, assuming zero polarisation and ground station tracking losses. For item (ii), since there is no attitude control system on-board i-INSPIRE[3], if we assume an average polarisation loss of 50% to the signal, we have a further 3 dB of attenuation and hence the link margin on average at the visible horizon is 3 dB. It was also calculated that when the satellite is vertically above the ground station (the closest i-INSPIRE gets to the ground station in orbit) the link margin is approximately 19 dB, and the average link margin for a given sighting is approximately 9 dB. This shows that i-INSPIRE will on average be able to be detected as long as the satellite is visible (line-of-sight) to the ground station.

Once communication access is made to i-INSPIRE, the transceiver and ground station must work together to transfer data (for more details regarding communication protocols, see Xiao et al. [3]). The transceiver on board the satellite can transmit at a maximum of 5 kilo bits per second (kbps). Taking into account the data transmission rate and the communication windows with i-INSPIRE, calculations show that the satellite can transmit around 1 mega byte (MB) of data per day. This is enough for approximately 40 spectral images (each image containing 8 individual spectra, and therefore 320 individual spectra in one day) or 50 VGA JPEG images of the Earth. (The amounts of housekeeping data are negligible in comparison.) This estimate assumes a 16:1 JPEG compression ratio. For more information on the images and scientific instruments, see Betters et al. [2].

[3]Satellite attitude simulations are currently being undertaken and will be used to get a better estimate of the time varying attitude of i-INSPIRE.

VII. Conclusion

This paper has described the engineering-specific aspects of i-INSPIRE. In particular, the aspects discussed were the design (0.75 kg tube-shaped pico-satellite), testing (vacuum, radiation, vibration and thermal), launch (IOS Neptune 45 from an offshore platform), orbital characteristics (310 km polar Earth orbit with a predicted lifetime of 24 days), and operation (dedicated ground station at the University of Sydney) of i-INSPIRE. The three onboard instruments (novel miniature spectrograph "NanoSpec", a radiation counter, and an imaging camera) were mentioned and further sources of information given. i-INSPIRE is intended to be a technology and capability demonstrator that points a way towards future, larger, Australian satellites.

VIII. Acknowledgments

The authors would like to thank Roderick and Randa Milliron of IOS for their documents on the launch vehicle, and their answers to various questions sent by e-mail.

References

[1] Fogarty, L., Cairns, I.H., Bland-Hawthorn, J., Wu, X., Betters, C., Funamoto, J., Leon-Saval, S.G., Monger, A.G. and Xiao, S., "The initial - INtegrated SPectrograph, Imager and Radiation Explorer (i-INSPIRE) - a university satellite project.", *Proceeding of the 11th Australian Space Science Conference*, 2011

[2] Betters, C., Cairns, I.H., Bland-Hawthorn, J., Wu, X., Fogarty, L., Funamoto, J., Leon-Saval, S.G., Monger, A.G. and Xiao, S., "Instrumentation of the i-INSPIRE satellite.", *Proceeding of the 11th Australian Space Science Conference*, 2011

[3] Xiao, S., Wu, X., Cairns, I.H., Bland-Hawthorn, J., Betters, C., Funamoto, J., Leon-Saval, S.G., Fogarty, L., Monger, A.G. and Bai, X., "i-INSPIRE Tube-Satellite Bus Design", *Proceeding of the 11th Australian Space Science Conference*, 2011

[4] Interorbital Systems, *TUBESAT PERSONAL SATELLITE KIT ASSEMBLY GUIDE, RELEASE 1.1*, 2009-2010 Interorbital Systems, Mojave, California, ios@interorbital.com

[5] Larson, W.J. and Wertz, J.R. (editors), *Space Mission Analysis and Design*, 1999, Third Edition, 2005, Space Technology Library

[6] Interorbital Systems, *PAYLOAD USERS GUIDE N45 Modular Rocket*, Interorbital Systems, Mojave, California, ios@interorbital.com

Space photonics: next generation space instrumentation

S.G. Leon-Saval[1] & J. Bland-Hawthorn[1,2]
[1]*Institute of Photonics & Optical Science (IPOS)*
[2]*Sydney Institute for Astronomy (SIfA)*
School of Physics A28, University of Sydney, NSW 2006, Australia

Summary: Recent developments in astrophotonics herald a new era for ground-based astronomy. These technologies are now being extended and adapted to space-borne instrumentation over the coming decade. One of the revolutionary developments is the photonic integrated multimode microspectrograph (PIMMS) that greatly reduces the size of any spectrograph, independent of the telescope aperture, the slit aperture or the spectroscopic resolution of the instrument. We now extend these ideas to space instrumentation where a much broader spectral range can be explored. We are focusing our efforts on the UV to mid-infrared (0.15-15μm) window that is increasingly becoming more accessible to photonic technologies.

Keywords: space photonics, astrophotonics, space sciences, astronomy

Introduction

During the period 1999-2002, our team in Australia worked on the development of optical/IR laser communications in space to vastly increase the data rates from satellite missions [1,2]. The idea here was to exploit the many small astronomical telescopes that were widely regarded as having passed their prime in order to assist vastly higher data download rates from ESA and NASA satellites. This led to the Centre for Space Photonics (www.aao.gov.au/lasers) which was established with a view to exploiting the huge investment in photonic technologies. Extended conversations with NASA led to a workshop at the Jet Propulsion Laboratory (2002) and a Special Session at the IAU General Assembly in Sydney (2003). In the years that followed, ESA and NASA, both of whom have their own long-standing developments, successfully demonstrated the viability of Gbs data-rate interplanetary transmissions [e.g. 3].

This early work convinced us of the huge potential that photonics would bring to the development of astronomical instruments, an international field we now know as astrophotonics [4]. This has already led to a number of remarkable new photonic technologies (e.g. Fig. 1): the integrated beam combiner [5], the aperiodic ultra broadband Fibre Bragg Grating (FBG) [6], the photonic lantern [7,8,9], the multicore FBG [10], the hexabundle [11], the 3D fan-out and 3D photonic lantern [12,13], the photonic microspectrograph [14,15], the vortex coronograph [16,17], inter alia. All of these devices are now being realized in astronomical instruments on ground-based telescopes.

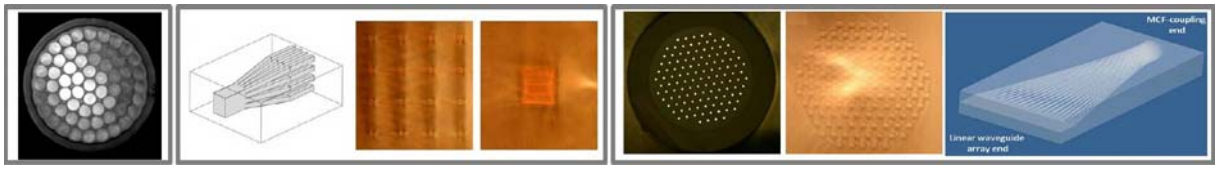

Fig.1.(left panel) Optical photograph of a 61 core Hexabundle. (middle panel) Schematic representation of a 3D photonic lantern and optical images of the endfaces; (right panel) multicore fibre and 3D fan-out device transforming a 2D core hexagonal array into a 1D core array for interfacing to a spectrograph.

In 2010, the Australian government announced funding in space science for the first time. We now propose to expand the field of space photonics to include the many new exciting capabilities that have arisen from astrophotonics. In fact, there are existing parallels already in place, including adaptive optics and laser metrology. Later this year our group at the University of Sydney will launch its first photonic fibre-based microspectrograph on a TubeSat. The i-INSPIRE TubeSat satellite shown in Fig. 2 [18,19], a pico-satellite (<1 kg) which will be the first to be built, launched and operated by a single Australian university. This is to be followed by CubeSat and a balloon-borne instrument in 2012-2013.

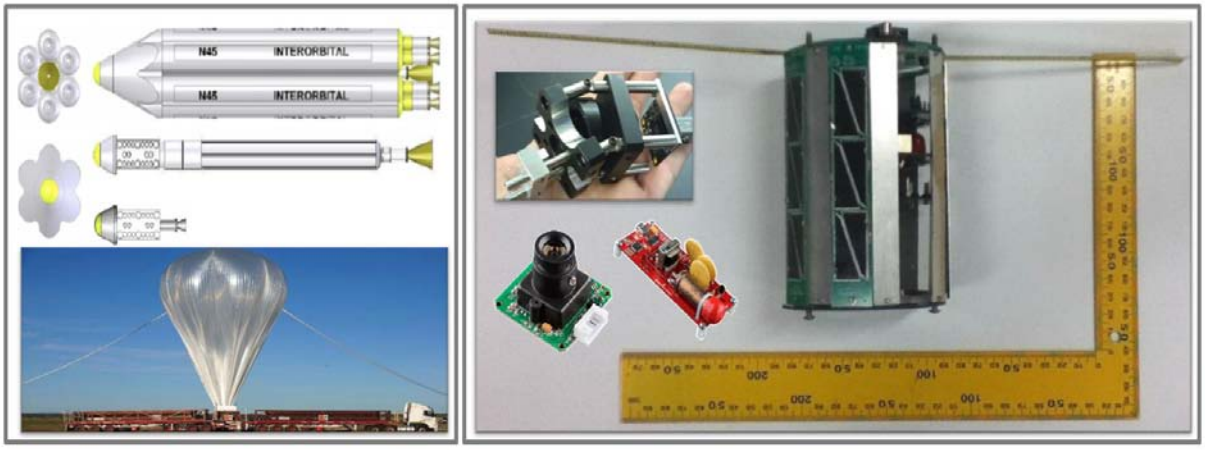

Fig.2. (left panel) Top image: Neptune 45 (N45) rocket developed by the United States company Interorbital Systems (IOS) that will launch the i-INSPIRE satellite in 2012-2013. Bottom image: NASA balloon launch. (right panel) Optical photograph of the actual i-INSPIRE satellite; inserts of the three different satellite payloads: a fibre-based microspectrograph (NanoSpec), a radiation counter and an imaging camera.

The Domain of Space Photonics

The Earth's atmosphere is a major limitation to ground-based observations, and completely opaque in certain wavebands (e.g. extreme UV, gamma rays). This has led to a veritable armada of space-borne observatories since the 1960s in order to explore new spectral (energy) domains.

The photonic revolution has been fuelled by the telecom industry, although its huge financial investment is almost entirely focused on a narrow spectral window near 1.5μm. Astrophotonics has expanded this window to 0.4-2.2 μm. However, we consider the window accessible to space photonics to be much broader, specifically two decades in wavelength centred at the C band (0.15-15 μm). This spectral window is of great interest to remote sensing, astrophysics, planetary and space science.

There are many challenges in photonics at both extremes of this wavelength range. Fibres with good UV response (over short lengths) are commercially available down to at least 0.2μm. Chalcogenide fibres and materials find use in space optics providing a good performance up to 15μm [20,21]. Both ends of this wavelength range can also be exploited by using hollow core fibres [22,23], where the absorption limitations of the material can be overcome. Further material and photonic developments at mid-IR and UV wavelengths are already being explored by Centre of Ultrahighbandwidth Devices for Optical Systems (CUDOS) and the Institute of Photonics and Optical Sciences (IPOS), both based at the University of Sydney.

Space Hazards

For the photonics technology to be useful for space applications, it must be able to withstand one of the harshest environments, namely, space. The space environment includes extremely low pressures, liquid helium to liquid nitrogen temperatures, as well as vast amounts of radiation and particles [24,25]. Furthermore, the extreme launching conditions such as vibration levels should be also considered. Test standards are well defined in the literature fuelled by the extensive studies in current standard photonics technologies deployed on space to date, such as fiber optic networks, laser diodes and detectors [26]. In the 1990s, the NASA COBE satellite first detected fine structure in the cosmic microwave background. For this groundbreaking work, the Nobel Prize in Physics was awarded to John Mather and George Smoot. What is not widely known is that large-core multimode fibres aboard the spacecraft almost sabotaged the experiment [27]. Charged particles passing through the satellite produced Cerenkov flashes within the fibres which overloaded the system. These same particles can interact destructively with on-board electronics and other components. This fact is well known to space agencies who carry out extensive radiation testing on payloads prior to launch. In collaboration with the Medical Physics group at the School of Physics, local medical facilities and nuclear physics labs, we are engaged in detailed radiation testing of all components that make up a space photonic instrument.

Microspectrographs

Photonics has advanced from the historic bulk-optic systems that were organized on an optical bench using many separate optical components, to relatively compact fiber-optic and integrated-optic devices that can combine several optical functions on one fiber or waveguide substrate. Integrated photonic technologies offer significant improvements in terms of manufacturing, size, weight, processing speed and power consumption over distributed bulk and micro-optic systems. This technology is ideal for use in harsh environments – e.g. space - as optical chips and fibres are compact, light weight, and as a result of the monolithic nature, highly robust.

It has long been recognized that highly integrated miniature spectrometers have many advantages for remote sensing and interplanetary science [28]. But there has been a sense that small spectrographs are fundamentally limited in terms of the observational parameter space (e.g. spectroscopic resolution) that is accessible to them. The revolutionary PIMMS concept has swept aside this limitation [15] (Fig. 3).

A completely general expression for the resolving power R of an ideal dispersing element is $R = \lambda/\delta\lambda = mN$ where N is the number of combining beams (or finesse) and m is the spectral order of interference. But this is only achieved in practice for diffraction-limited instruments. A simple illustration serves to demonstrate how far astronomical instruments fall short of this ideal. Consider a spectrograph with a grating line density of ρ = 1000 lines mm^{-1} placed at a pupil with diameter, say, D_{pup} = 50 mm. In a perfect system, for a flat pupil illumination, the peak spectral resolving power is then $R = m\rho D_{pup}$ = 50,000 where we adopt the simplest configuration for which m = 1. Diffraction-limited optical lenses are commercially available such that the overall length of the instrument is roughly $L \sim 4FD_{pup}$, or about 40 cm in length (F=2). This is much smaller than any large aperture, broadband spectrograph working at such high resolution and, furthermore, these other instruments operate typically at $m > 1$ to achieve higher resolving power.

The importance of striving for an ideal system can be seen by expressing the resolving power as $R = \varepsilon mN$ where ε is the factor (ε<1) by which a spectrograph falls short of the ideal

in terms of the number of combining beams available to the designer in a diffraction-limited system. An ideal instrument can be made a factor of $1/\varepsilon$ smaller in linear extent to achieve a given resolving power R. A review of widely used seeing-limited spectrographs reveals that ε ~ 0.003-0.03.

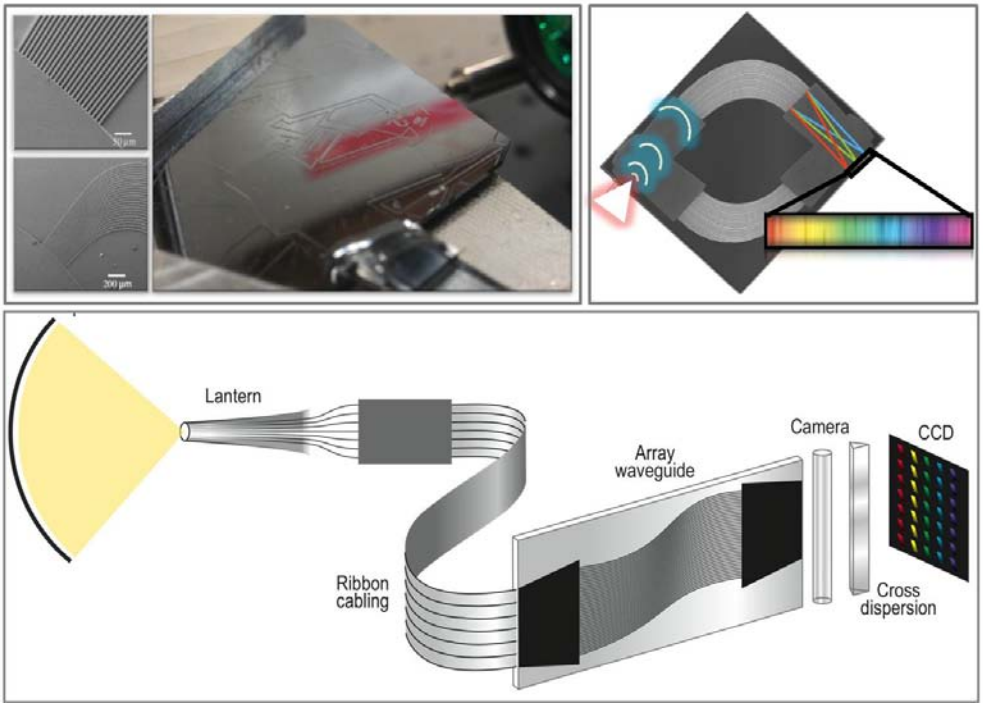

Fig.3. PIMMS concept [15]: (top left panel) optical photograph and scanning electron microscope images of a Arrayed Waveguide Grating (AWG) device use as the dispersive element for the microspectrograph; (top right panel) Schematic of the AWG working principle (image courtesy of N. Cvetojevic); (bottom panel) the photonic lantern accepts incoherent light and converts it to single-mode propagation and a set of diffraction limited point spread functions (i.e. single-mode fibres) aligned along a slit to couple into an AWG that serves as the dispersive element. Here we show an asymmetric rather than a folded AWG [14].

So why are spectrographs so large? A spectrograph matched to a perfect telescope can be reduced to its diffraction-limited, minimum configuration (ε=1, m=1). But at optical and near-IR wavelengths, AO systems fall short of the diffraction limit. However, with the aid of a remarkable device, known as the photonic lantern, even an aberrated psf from an imperfect AO system can be efficiently matched to a minimum configuration spectrograph (Fig. 1). Finally, we find that *any* source of incoherent illumination can also be matched to a minimum configuration spectrograph. A by-product of our solution is that incoherent light from a fast input beam (F≥2) can be fed to a spectrograph with an arbitrarily high resolving power.

Conclusion

This leads us a new way of thinking about spectrometers. We can separate the performance of the telescope and/or entrance aperture from the performance of the instrument. We can now speak of compact diffraction-limited integrated photonic instruments regardless of the source of illumination. This has major implications for the cost of developing and building space instruments. But then nothing comes for free. Our radical approach requires a new generation

of high-performance, small pixel detectors. The minimum configuration spectrograph is expensive in its use of detector pixels, but the cost is manageable.

Acknowledgements

The authors would like to thank the i-INSPIRE team for their effort, useful discussions and ideas. The i-INSPIRE team are: Prof I. Cairns (project leader), Dr L. Fogarty, Dr X. Wu, Mr. C. Betters, Mr. J. Funamoto, Dr T. Monger, and Mr. S. Xiao. SLS is supported by an Australian Research Council Australian Postdoctoral Fellowship. JBH is supported by an Australian Research Council Federation Fellowship.

References

1. Harwit, A., Bland-Hawthorn, J., and Harwit, M., "Laser Telemetry to Increase Astronomical Downlink Capacities," 2003, Publications of the Astronomical Society of the Pacific, 115, 720-724
2. Bland-Hawthorn, J., Harwit, A., and Harwit, M., "Laser Telemetry from Space," 2002, Science, 297, 523
3. Smith, D.E. et al, "Two-way Laser Link over Interplanetary Distance," 2006, Science, 311, 53
4. Bland-Hawthorn, J. and Kern, P., "Astrophotonics: a new era for astronomical instruments," 2009, Optics Express, 17, 1880-1884
5. Kern, P., Le Coarer, E., and Benech, P., "On-chip spectro-detection for fully integrated coherent beam combiners," 2009, Optics Express, 17, 1976-1987
6. Bland-Hawthorn, J., Englund, M., and Edvell, G., "New approach to atmospheric OH suppression using an aperiodic fibre Bragg grating," 2004, Optics Express, 12, 5902
7. Leon-Saval, S.G., Argyros, A., and Bland-Hawthorn, J., "Photonic lanterns: a study of light propagation in multimode to single-mode converters," 2010, Optics Express, 18, 8430
8. Leon-Saval, S.G., Birks, T.A., Bland-Hawthorn, J., and Englund, M., "Multimode fiber devices with single-mode performance," 2005, Optics Letters, 30, 2545-2547
9. D. Noordegraaf, P. M. Skovgaard, M. D. Nielsen, and J. Bland-Hawthorn, "Efficient multi-mode to single-mode coupling in a photonic lantern," Opt. Express **17**, 1988-1994 (2009).
10. Birks, T.A. et al, “Fibers are Looking Up: Optical Fiber Transition Structures in Astrophotonics” 2010, Frontiers in Optics, paper FTuU1
11. J.J. Bryant et al, "Characterization of hexabundles: initial results” Monthly Notices of the Royal Astronomical Society Volume 415, Issue 3, pages 2173–2181, August 2011
12. Thomson, R.R. et al, "An Integrated Fan-out Device for Astrophotonics," Frontiers in Optics 2010, PDP
13. Thomson, R. R., T. A. Birks, S. G. Leon-Saval, A. K. Kar, and J. Bland-Hawthorn, "Ultrafast laser inscription of an integrated photonic lantern," Opt. Express 19, 5698-5705 (2011)
14. Cvetojevic, N. et al, 2009, "Characterization and On-Sky Demonstration of an Integrated Photonic Spectrograph for Astronomy,” Optics Express, 17, 18643-18650
15. Bland-Hawthorn, J., and 10 colleagues, "PIMMS: photonic integrated multimode microspectrograph," 2010, Society of Photo-Optical Instrumentation Engineers (SPIE) Conference Series, 7735
16. Mawet, D., and 5 colleagues, "The Vector Vortex Coronagraph: Laboratory Results and First Light at Palomar Observatory," 2010, Astrophysical Journal, 709, 53-57

17. Mawet, D., and 6 colleagues, "Optical Vectorial Vortex Coronagraphs using Liquid Crystal Polymers: theory, manufacturing and laboratory demonstration," 2009, Optics Express, 17, 1902-1918
18. L. Fogarty, I. Cairns, J. Bland-Hawthorn, X. Wu, C. Betters, J. Funamoto, S. G. Leon-Saval, T. Monger, , and S. Xiao, "The initial-INtegrated SPectrograph, Imager and Radiation Explorer (i-INSPIRE) - a university satellite project." in Proceeding of the 11th Australian Space Science Conference, 2011.
19. C. Betters, I. Cairns, J. Bland-Hawthorn, X. Wu, L. Fogarty, J. Funamoto, S. G. Leon-Saval, T. Monger, and S. Xiao,"Instrumentation of the i-INSPIRE satellite," in Proceeding of the 11th Australian Space Science Conference, 2011.
20. A. A. Wilhelm, Boussard-Plédel, Q. Coulombier, J. Lucas, B. Bureau, P. Lucas,"Development of Far-Infrared-Transmitting Te Based Glasses Suitable for Carbon Dioxide Detection and Space Optics." Advanced Materials, Volume 19, Issue 22, pages 3796–3800, November, 2007
21. S. Danto, P. Houizot, C. Boussard-Pledel, X.-H. Zhang, F. Smektala, J. Lucas, "A Family of Far-Infrared-Transmitting Glasses in the Ga–Ge–Te System for Space Applications," Advanced Functional Materials Volume 16, Issue 14, pages 1847–1852, September, 2006.
22. Yoel Fink, Joshua N. Winn, Shanhui Fan, Chiping Chen, Jurgen Michel, John D. Joannopoulos and Edwin L. Thomas, "A Dielectric Omnidirectional Reflector," 1998, Science, Vol. 282 no. 5394 pp. 1679-1682.
23. Sébastien Février, Frédéric Gérôme, Alexis Labruyère, Benoît Beaudou, Georges Humbert, and Jean-Louis Auguste, "Ultraviolet guiding hollow-core photonic crystal fiber," Opt. Lett. 34, 2888-2890 (2009)
24. M. Kruglanski, E. de Donder, N. Messios, E. Gamby, L. Hetey, S. Calders, and H. Evans, "SPENVIS – Space Environment, Effects, and Education System," spenvis.oma.be, 2011.
25. E. R. Benton and E. V. Benton, "Space radiation dosimetry in low-Earth orbit and beyond," Nuclear Instruments and Methods in Physics Research B, vol. 184, pp. 255–294, sep 2001.
26. http://photonics.gsfc.nasa.gov/
27. J.C. Mather, personal communication to JBH in 2010.
28. A. Scott, N. Rowlands, A. Bell, Miniature spectrometers for planetary remote sensing, Proc. SPIE 5660, pp. 78-87, 2004.

Electric (ion) propulsion devices for satellites of any size: The Charge Exchange Thruster (CXT)

Jiro Funamoto*†, Joe Khachan*, Xiaofeng Wu†, Adam Israel* and Rishi Verma†

* *School of Physics, The University of Sydney, NSW, 2006, Australia*
† *School of Aerospace, Mechanical and Mechatronic Engineering, The University of Sydney, NSW, 2006, Australia*

Summary: An emerging electric propulsion system, the Charge Exchange Thruster (CXT) is discussed. The CXT is an electric powered ion propulsion system, providing thrust by the acceleration of ions along a potential difference on the order of 15 kV. The novel characteristic of the CXT is the need to no longer neutralise the exhaust particles. This is because the accelerated ions in the CXT undergo charge exchange reactions, thereby already resulting in an exhaust of neutral particles. This internal and implicit neutralisation of the accelerated ions gives the CXT a large advantage over conventional designs that require large electron guns to neutralise the exhaust ions. The CXT also has an extremely simple and robust design. These characteristics allow the CXT to be miniaturised to extremely small sizes like a pencil. Current CXTs have produced 86 μN at 0.4 W of power. Applications include orbital station-keeping, manoeuvring and orbital maintenance. Such small thrusters could be used on nano-satellites to prevent orbital decay and extend their lifetime from a matter of weeks to the order of years.

Keywords: propulsion, thruster, ion, satellite, electric, nano, plasma, neutralisation

I. Introduction

Electric propulsion in this paper refers to the spacecraft propulsion technology using electricity as the main power source. When compared to other forms of spacecraft propulsion (e.g. chemical), electric propulsion is typically characterised by low thrust but extremely high fuel efficiency [1]. Electric propulsion is beneficial for long duration missions and for orbital station keeping where fuel efficiency is a necessity. This paper will describe a new type of electric propulsion device, the Charge Exchange Thruster (CXT) which uses a simple and novel plasma mechanism (charge exchange) to achieve an electric propulsion device which can be scaled down in physical size to one befitting a pico- or nano-satellite. The CXT was invented by the Fusion Group in the School of Physics at the University of Sydney, and is now pursued as a collaborative project with the School of Aerospace, Mechanical and Mechatronic Engineering also at the University of Sydney. To appreciate the full advantage of the CXT over other forms of propulsion (specifically other available electric propulsion systems) the basics of electric propulsion and the problems faced by commercially available electric propulsion systems will be outlined in this introduction section before describing the novel propulsion device, the CXT.

Basics of electric propulsion over chemical propulsion

Electric propulsion is a propulsion technology using electrical energy as the main power source, whereas chemical propulsion uses chemical energy as the main power source. The propellant on the other hand is the same for both "propulsion devices" ("thrusters" we will call these) and embodies the high speeds gas particles exiting the thruster. It is only through the propulsion of propellant particles in the backward direction that an equal and opposite momentum is transferred to the thruster in the forward direction. The thruster is therefore simply a device which takes energy from the power source and transfers it to the propellant particles (which impart their momentum to the thruster along the direction they are propelled).

Again, it must be stressed that the power source and the propellant should be considered as two distinct entities; this is indeed the case for electric thrusters, but is not for chemical thrusters. This will help in understanding why the kinetic energy of the propellant particles can be increased for electric thrusters but must stay effectively constant for chemical thrusters; a property that allows electric propulsion to theoretically be many orders of magnitude more fuel efficient than chemical thrusters.

In an electrical thruster, the power source and propellant are two distinct entities. The power source is often a battery or electrical generator on the spacecraft whereas the propellant is a gas. The gas is ionised and accelerated through a electric potential difference, transforming electrical energy to kinetic energy of the propellant. It is thus evident that an increase in particle energy (and hence momentum transferred to the thruster) can be easily gained by accelerating the propellant across a larger potential difference.

On the other hand, in a chemical thruster (such as a typical "rocket") the power source is the chemical energy acquired from the breaking of chemical bonds, and the propellant is the constituents and products of the chemical reaction. The power source and propellant are therefore part of a single entity, the initial fuel-oxidiser mixture. From this property, it can be deduced that an increase in kinetic energy of each propellant particle is difficult to obtain. This is because to increase the energy of the propellant particles, more chemical energy is needed. However, to attain more chemical energy, more fuel-oxidiser must be burnt, proportionally increasing the number of particles the total chemical energy must be shared amongst. In the end, burning more fuel-oxidiser in the combustion chamber in general does not change the energy per propellant.

Whether the kinetic energy of each propellant particle can be changed determines the fuel efficiency of the thruster and is therefore of extreme importance. This is because the kinetic energy determines the exit velocity of the propellant particles, which in turn is a measure of the fuel efficiency (a measure of the momentum attained by the thruster/spacecraft per mass of fuel spent) of a propulsion system. The higher the exit velocity (and hence kinetic energy) the greater the fuel efficiency. This is evident by considering that any total change in momentum of the satellite Δp must be composed of small momentum contributions from each propellant particle (of which we will assume for this argument to be a single atomic species of mass m and average velocity v); thus $\Delta p = Nmv$, where N is the total number of particles needed for the total change in momentum Δp. To minimise the number of propellant particles N spent for a given change in thruster/spacecraft momentum Δp it is seen that the exit velocity (and hence the kinetic energy) of the propellant particles must be as high as possible. Unlike chemical thrusters, electric thrusters allow acceleration of the propellant

particles to theoretically any subluminal velocity (by increasing the potential difference along which the particle is accelerated), and therefore can theoretically attain orders of magnitude higher fuel efficiencies than chemical thrusters.

The downside is that increasing the kinetic energy of the particles requires more electrical power from the spacecraft. In space however, fuel efficiency is often of more importance, as electrical energy is renewable (through solar panels) whereas fuel is not; this is an even greater consideration for long duration or deep space missions.

Problems with existing electric propulsion units

There are three major issues with existing propulsion units which limit their lifetime and performance. These problems will be described here so they can be addressed in the following section about the CXT. Although there are various types of electric propulsion, the main focus of this paper will be ion propulsion (propulsion attained by accelerating ions over a nominally static potential difference). Ion propulsion has been studied for more than 50 years and the two main systems currently available commercially are the Gridded Ion Thruster (GIT) and the Hall-Effect Thruster (HET) [1].

The first issue with existing thrusters is the limit on the lifetime of the thruster due to physical erosion of the thruster components by high energy propellant ions. In both the GIT and HET systems, ions are accelerated across a potential difference on the order of kV and these ions can cause physical erosion to components which lie in the path of the accelerated propellant. For the GIT, the accelerating grid(s) (which is a physical mesh in the path of the propellant plume, providing the potential difference needed for propellant acceleration) undergoes erosion. For the HET, despite an absence of a physical accelerating grid, the interior ceramic erodes, limiting the lifetime of the HET [1].

The second issue is that although the GIT and HET are electric thrusters, they can not completely attain the full benefit of electric propulsion; the full benefit of electric propulsion being the ability to accelerate the propellant to any subluminous velocity and thereby reaching the highest of fuel efficiencies. For the GIT, this is because the acceleration potential difference can not be increased over approximately 5 kV, as a further increase causes much increased grid erosion. For the HET, the source of the potential difference is a cloud of trapped electrons, and increasing their density and hence bulk potential difference is difficult past a particular voltage [1]. These limits on the potential difference (and hence propellant exit velocities) attainable in the GIT and HET designs place a cap on the maximum fuel efficiency possible with these thrusters.

The third issue with the GIT and HET is that they require an external neutralisation source. This external neutralisation source sprays electrons into the propellant plume neutralising the outgoing propellant (ions). If this is not done, 1) the particles will pull the thruster back in the opposite direction, 2) the thruster will attain a large opposite charge over time (this also results in pulling all particles back on to the spacecraft, and other undesirable effects). To neutralise the exiting particles, the GIT and HET designs both use external electron guns, which may be heavy and/or bulky [1].

II. Overcoming existing problems: The Charge Exchange Thruster (CXT)

The Charge Exchange Thruster (CXT) is an electric thruster which addresses all three main limitations of existing systems mentioned above by relying on a plasma phenomenon novel to electric propulsion systems, charge exchange. The CXT does not use accelerating grids or a ceramic interior, is not limited to a few kV (15 kV thrusters have been tested) allowing greater fuel efficiency, and does not require an external neutralisation source as the exiting particles are already neutral (through charge exchange reactions). The subsections below will outline 1) the physical characteristics and 2) the physics of operation of the CXT.

Physical characteristics of the CXT

The CXT designs created so far are tubular in shape and consist of a hollow insulating tube separating an anode plate covering one end and a funnel-shaped cathode (nozzle) on the other (Fig. 1). A gas feed must be present somewhere in the thruster and is present on the back anode plate for the thruster in Fig. 1. The thruster must have relatively air tight (hermetic) seals between the insulating tube and the cathode/anode (electrodes), with the only exit for particles being the hole in the cathode nozzle. The anode is usually at ground potential and the cathode charged negative up to (and over) 15 kV; more on the operation in the proceeding subsection.

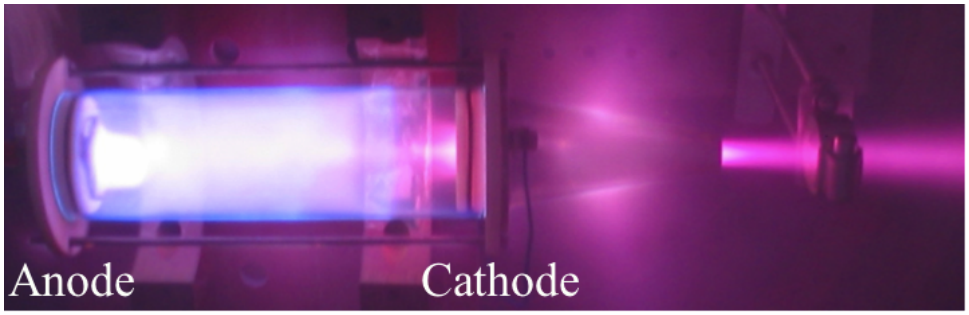

Fig. 1: An old CXT prototype in operation. The length of the thruster is approximately 20 cm, with a diameter of 4 cm. The anode plate and cathode cone are made from steel. The insulating tube separating the anode and cathode is made from glass, allowing an inside view of the thruster in operation.

Newer designs of the CXT have seen miniaturisation to extremely small sizes, smaller than a pen. One such thruster can be seen in Fig. 2. The length of this miniaturised CXT is only 5 cm, with an internal diameter of approximately 1 cm.

Small versions of the CXT are less than 50 grams in mass and allow its use in extremely small satellites such as nano- or pico-satellites (such as the relatively common 1 kg “CubeSat” series satellites). Even smaller versions are currently being developed and tested at the University of Sydney. To current knowledge, the operation of the CXT thruster is not affected by miniaturisation of the thruster, as long as pressure and voltage scaling is applied to maintain effectively the same plasma dynamics inside the thruster. The plasma dynamics of the CXT will be explained in the following subsection about the physics of operation.

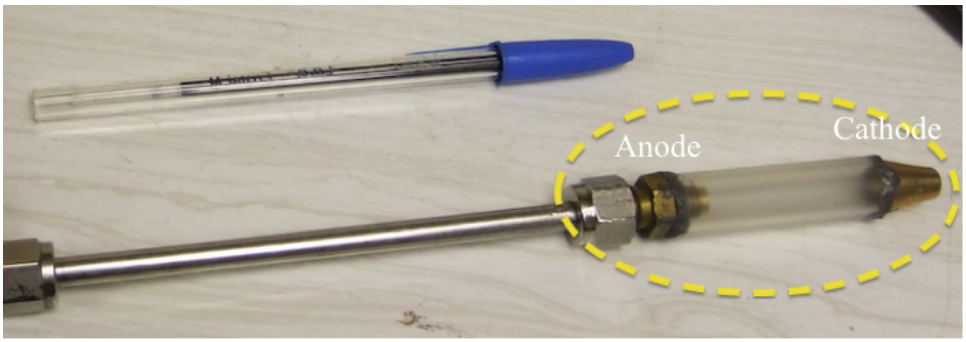

Fig. 2: Miniaturised CXT. The CXT is the device enclosed by the yellow dashed line. Anode and cathode made from brass and insulating tube from an opaque fused quartz glass tube. The steel pipe connected to the CXT is a gas feed pipe.

The physics of operation

A schematic of the essential elements of the CXT is shown in Fig. 3 (note: this schematic does not show the gas feed, but should be present somewhere in the thruster). The CXT is operated in a vacuum environment. Neutral gas particles (hydrogen and argon have been tested) are pumped into the CXT chamber at a mass flow rate of a few standard cubic centimetres per minute (sccm), and a potential difference is applied between the anode and cathode. The anode is usually at ground potential and the cathode at a voltage up to -15 kV.

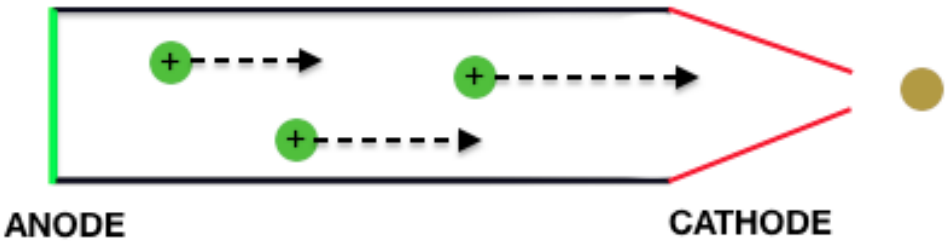

Fig. 3: A schematic of the essential elements of the CXT. Note that there should be a gas feed to the inside of the thruster, but is not shown here. The anode is usually at ground potential, and the cathode at a voltage up to -15 kV relative to ground potential.

With the application of a potential difference, some of the neutral gas ionises into ions and electrons. The ions and electrons are accelerated across the potential difference, causing further ionisation in the neutral background gas in the thruster. Somewhere along the flight of the ion, the ion undergoes a charge exchange reaction with a neutral background gas particle. Charge exchange is the process in which an ion and neutral gas particle come sufficiently close that an electron on the neutral gas particle finds it more energetically favourable to bind to the ion. This interaction therefore changes a high energy ion and slow neutral to a high energy neutral and slow ion. The high energy neutral (former ion) is then able to exit the hole in the cathode without being attracted to the cathode itself.

The presence of high energy neutrals exiting the thruster was first confirmed with spectroscopy of the light emitted out of the cathode nozzle of the thruster. The energy of the

neutrals have been measured using the technique of Doppler spectroscopy and found to correspond to up to 90% of the applied potential difference [3].

The complete details of operation of the CXT is not yet fully understood. A comprehensive theoretical model is also not yet available. However, neutralisation of high energy ions via charge exchange reactions is thought to be the predominant reaction responsible for the ejection of neutrals from the thruster. This is due to the fact that charge exchange reactions are the predominant neutralisation phenomenon for a plasma with energy and density parameters close to that operated within the CXT [3, 4].

It is interesting to note that the results from Doppler spectroscopy show that the ion undergoes charge exchange mostly within the cathode nozzle rather than in the volume of the thruster before the nozzle. This could be due to the charge exchange cross section being greater for higher energy ions (highest energies ion are found closer to the cathode where they have had maximal acceleration through the potential difference of anode to cathode), or due to the possible setup of a virtual anode space charge within the cathode nozzle (discussed in Israel et al. and Blackhall et al. [2, 3, 4]).

Although a comprehensive theoretical model is yet to be devised and will be future work in this area, a variety of analysis techniques, including Langmuir probes and Doppler spectroscopy have been used by Israel et al. and Blackhall et al. to analyse the physics of the CXT and have supported the present model of charge exchange reactions. Other evidence which supports this model is empirical evidence from results of spectroscopy and thrust measurement experiments as described in the following section.

III. Thrust measurements and efficiency

The thrust produced by the CXT has been measured using a torsional balance, called a momentum transfer pendulum (MTP) which deflects under the action of a force (for further details see Israel et al. [3]). The measurement plate of the torsional balance (the MTP) is placed in the path of the thruster propellant plume and the deflection of the balance is measured and compared against a calibration chart of deflection to force (see Fig. 4). These thrust measurements constitute indirect thrust measurements as the MTP measures the momentum of the plume of the thruster and indirectly deduces the force on the thruster, rather than measuring the force on the thruster directly. This method was used because it is extremely difficult to perform μN level direct thrust measurements on the thruster (mainly due to frictional forces caused by the gas pipe or high voltage leads attached to the thruster, and any bearings supporting the thruster). Therefore, all thrust measurement results come from indirect thrust measurements using a MTP. Future studies will venture at performing direct thrust measurements.

The thrust from a 12 cm long, 1.5 cm diameter miniaturised CXT (Fig. 4) was measured. This CXT can be seen connected to the gas feed (blue pipe) and the necessary electrical connections in Fig. 4. The MTP can be seen on the other side of the aluminium plate. The aluminium plate electrostatically shields the charged cathode to the measurement plate of the MTP, which without electrostatic shielding would cause movement of the plate by electrostatic forces during operation. There is a small hole in the aluminium plate which allows the thruster plume to hit the MTP. A laser shone on the other side of the MTP is used to determine the

deflection of the plate accurately. The CXT was operated in a vacuum environment at a pressure of around 10^{-5} torr (or 10^{-3} Pa).

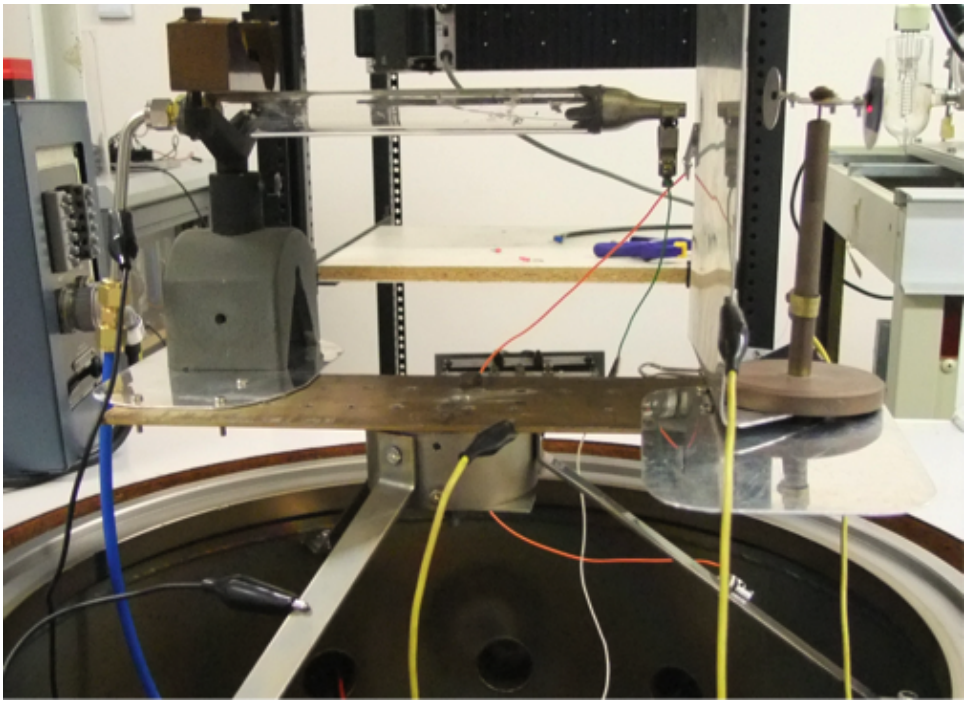

Fig. 4: Photograph of the 12 cm long, 1.5 cm diameter CXT used for obtaining the thrust measurements found in this paper. The CXT is on the left and the MTP is on the right. An aluminium plate is used to electrostatically shield the CXT cathode from the MTP measurement plate.

Results obtained from the CXT described above constitute the most recent measurements of a CXT (the 12 cm long, 1.5 cm diameter CXT). For these measurements two different gases were tested, hydrogen and argon. Note that we expect higher thrust from argon over hydrogen due to the approximately 40 times heavier mass, easier ionisation and higher charge exchange cross section of argon. It can be seen that these properties have also resulted positively in better power consumption, higher thrust and lower flow rate of the argon propellant CXT.

Table 1: Thrust produced by the most recent CXT (12 cm long, 1.5 cm diameter).

Gas	Mass flow rate [sccm]	Applied voltage [kV]	Power use [W]	Thrust [μN]
Hydrogen	7	12.5	2.7	18
Argon	<1	15	0.4	86

In both cases the specific impulse (a measure of the fuel efficiency of a propulsion system, equal to the change in momentum gained per unit weight of fuel spent) of the CXT was estimated by Doppler spectroscopy to be on the order of 10000 s (with hydrogen propellant having slightly greater and argon slightly lower values). This is over a factor of 2 larger than the GIT and HET conventional electric propulsion systems [1], and denotes a proportional factor of fuel efficiency over the GIT and HET systems. This can be attributed to the fact that the CXT is not limited in the voltage we apply, and we had applied voltages significantly greater than, and therefore attained propellant exit velocities substantially overwhelming that of typical GIT and HET systems.

This specific impulse value of 10000 s however has not taken into account the fuel expended from leakage of neutral gas from the hole in the cathode during operation. This property is yet to be measured accurately and will be an update in a future paper when determined. Currently, if all the fuel was coming out as energetic neutrals, then the exit velocity of the neutrals is such that the specific impulse would be the aforementioned approximately 10000 s. This denotes that the CXT may not be more fuel efficient than the GIT or HET designs depending on the neutral gas leakage rate from the cathode hole. This must be determined conclusively in a future study. Nonetheless, there is little change in the fact that 86 μN was attained for a power of 0.4 W using argon propellant, with fuel efficiency possibly greater than existing electric thrusters.

IV. Applications

The aforementioned low power requirements and small CXT sizes enable major applications in pico-, nano-, and micro-satellites (satellites of 0.1-1 kg, 1-10 kg, and 10-100 kg mass respectively). It is believed that currently no known efficient propulsion system exist for satellites in the 1-10 kg range. Nano-satellites such as the popular "CubeSat" series nano-satellites are often used by many educational institutions around the world. Many of these satellites enter low Earth orbits (LEOs) beneath approximately 500 km altitude where the atmospheric drag is still relatively significant such that the satellite could spiral back to Earth in a matter of weeks or months [5]. If a miniaturised CXT is flown on a nano-satellite in LEO, the CXT could possibly extend the lifetime of the satellite from a matter of weeks or months, to the order of years through orbital station-keeping. Furthermore, 0.4 W of power for the CXT is very reasonable even to the strict limited power budget of a nano-satellite, since typical solar panels of 10 cm^2 on a nano-satellite can produce more than 2 W of power when directed at the sun. Multiple CXTs can also being considered for increased thrust output and other manoeuvres such as accurate satellite attitude changes and satellite formation flying.

V. Current work and future directions

To develop the CXT to a space ready system many developments still need to take place. In particular, (1) the thrust as a function of power and gas consumption must be characterised, (2) the most efficient design (diameter, length, and cathode shape) of the CXT needs to be determined, and (3) the CXT must be made into a complete standalone space-ready system.

For item (1), although many experiments have been conducted and a general trend in thrust-power and thrust-fuel rate found, work still needs to be done in completely characterising the phenomena. In particular, it has been found recently that an optimum mode of operation exists for the thruster where applying a higher electric potential changes the plasma mode of operation and the measured thrust dramatically decreases. Such phenomena are yet to be studied completely.

For item (2), although a variety of thruster designs and sizes have been tested, it is of importance from a application standpoint to find the most efficient design. In this process, it is also of great interest to study the point to which the CXT can be shrunk before the plasma dynamics can no longer be reproduced.

Item (3) is the most important for the final space-ready thruster. The gas canister, high voltage converter (and possibly power supply), and the thruster itself must be integrated into a single device. Of particular importance is insulating the high voltage cathode from the remaining satellite electronics. To reduce the size of the gas canister, ablated or sublimated solid fuel could be used and their possibilities are currently being investigated.

VI. Conclusion

The CXT is a radical, novel electric propulsion system that solves the three main constraints of existing commercial electric propulsion systems. These conditions met are the absence of any eroding structure (such as an accelerating grid) increasing the thruster lifetime, unlimited application of voltage allowing extremely high fuel efficiency, and the absence of bulky neutralisation sources. Furthermore, the extremely simple design and absence of the neutralisation sources allows the CXT to be miniaturised to sizes smaller than a pencil. Such small and efficient propulsion systems have major applications in pico-, nano-, and micro-satellites, where efficient propulsion systems are underdeveloped and unknown.

References

[1] Goebel, D.M. and Katz, I., "Fundamentals of Electric Propulsion: Ion and Hall Thrusters", *Jet Propulsion Laboratory California Institute of Technology 2008, JPL SPACE SCIENCE AND TECHNOLOGY SERIES*, 2011

[2] Israel, A., "Investigations into the capabilities of the Charge-Exchange Thruster for applications in electric propulsion", *Department of Fusion Studies, School of Physics, University of Sydney*, 2011

[3] Israel, A. and Khachan, J., "Thrust measurements of a Charge-exchange Thruster", *Department of Fusion Studies, School of Physics, University of Sydney*, 2011

[4] Khachan, J. and Blackhall, L., "A simple electric thruster based on ion charge exchange" *Department of Fusion Studies, School of Physics, University of Sydney*, IEPC-2007-35, 17-20, 2007

[5] Verma, R., "The Development of a New Class of Electric Propulsion System: The Charge-Exchange Thruster (CXT)" *Thesis, School of Aerospace, Mechanical and Mechatronic Engineering, The Faculty of Engineering, University of Sydney*, 2011